Coordination Chemistry Reviews 253 (2009) 2959–2979

Contents lists available at ScienceDirect

Coordination Chemistry Reviews

journal homepage: www.elsevier.com/locate/ccr

Review

Two-dimensional molecular porous networks constructed by surface assembling

Hailin Liang, Yang He, Yingchun Ye, Xiaoguang Xu, Fang Cheng, Wei Sun, Xiang Shao, Yongfeng Wang, Jianlong Li, Kai Wu*

Beijing National Laboratory for Molecular Sciences, State Key Laboratory for Structural Chemistry of Unstable and Stable Species, College of Chemistry and Molecular Engineering, Peking University, No. 5 Yiheyuan Road, Haidian District, Beijing 100871, China

Contents

ARTICLE INFO

Article history:
Received 17 February 2009
Accepted 27 July 2009
Available online 7 August 2009

Keywords:
Molecular porous networks
Self-assembly
STM
van der Waals force
Hydrogen bonding
Metal–ligand coordination
Chemical bonding
Substrate effect
Solvent effect

ABSTRACT

In this review, we present an up-to-date account of various two-dimensional molecular porous networks that possess periodically arranged voids of different symmetries. These porous networks may be used as secondary templates to host guest ensembles. The size of the periodic voids and inter-void distance can be well below 10 nm that is hard to achieve with any other known techniques employed in nanoscience and nanotechnology. Moreover, the assembled voids may have various functional groups that can be chemically and biologically sensitive to specific ensembles. This makes the porous networks useful in preparing chemical and biological sensors. As the void size may be stepwise tuned at the scale that is comparable with the Fermi length of electrons, the confined space within the voids could serve as a spatial cavity for new chemical reactions. All these potential applications have driven people to develop various novel molecular porous networks. The tough challenges in all these efforts are associated with the controllability, predictability, stability and applicability of these porous networks. Numerous studies have led to the conclusion that the most efficient approach to fabricating these molecular porous networks is probably surface assembling of various functional organic molecules that form either uni-molecular or bi-molecular systems. The assembling process can be carried out either under ultrahigh vacuum conditions

Abbreviations: 2D, two-dimensional; BC16, 3,8-bis-hexadecyloxy-benzo[c]cinnoline; BDBA, 1,4-benzenediboronic acid; BTB, 1,3,5-benzenetribenzoic acid; DBA, hexadehydrotribenzo[12]annulene; DIP, di-indenoperylene; DPDI, 9-diaminoperylene-quinone-3,10-diimine; ECSTM, electrochemistry scanning tunneling microscope; F16CuPc, fluorinated copper-phthalocyanine; H_2-TBPP, 5,10,15,20-tetrakis-(3,5-di-tertiarybutylphenyl) porphyrin; HBs, hydrogen bonds; HHTP, 2,3,6,7,10,11-hexahydroxytriphenylene; HOPG, highly oriented pyrolytic graphite; LEED, low energy electron diffraction; ML, monolayer; MPNs, molecular porous networks; NEXAFS, near-edge X-ray absorption fine structure; OMBE, organic molecular beam epitaxy; PBP, 5,5′-bis(4-pyridyl)(2,2′-bipyrimidine); PTCDI, perylene tetra-carboxylic di-imide; SAMs, self-assembled monolayers; STM, scanning tunneling microscope; STS, scanning tunneling spectroscopy; TCB, 1,2,4-trichlorobenzene; TMA, trimesic acid (1,3,5-benzenetricarboxylic acid); TPA, terephthalic acid; TSB35, 1,3,5-tris [(*E*)-2-(3,5-didecyloxyphenyl)-ethenyl]-benzene; UHV, ultrahigh vacuum; vdW, van der Waals; XPS, X-ray photoelectron spectroscopy; ZnOEP, zinc octaethylporphyrin; ZnPc, zinc phthalocyanine.

* Corresponding author. Tel.: +86 10 62754005; fax: +86 10 62754005.
E-mail address: kaiwu@pku.edu.cn (K. Wu).

0010-8545/$ – see front matter
doi:10.1016/j.ccr.2009.07.028

or in liquid environments. The final assembling structures are actually balanced products of various interactions among the assembling molecules, substrates and/or solvents. In order to control and tune the porous network structures, one has to finely tweak these interactions. Among all the interactions, the inter-molecule interaction might be the most important. During surface assembling, non-covalent weak interactions are normally made use of to hold the molecules together. These weak interactions are typically fragile to external energy perturbations, which makes it extremely difficult to control and predict the assembled porous networks. In this context, we focus on the van der Waals force, dipole–dipole interaction, hydrogen bond and metal–ligand coordination and mainly describe various strategies utilized to tune these weak interactions so that specific molecular porous networks can be achieved in a controlled manner. Besides the inter-molecule interactions, we will also discuss effects of the substrates, solvents and external fields that could be used to realize the molecular porous networks. In addition to the non-covalent bonds, chemical bonds can be used to fabricate chemically stable porous networks too. After having discussed the issues described above, we will move on to introduce some applications of these porous networks. Finally, we will make summaries of the strategies and approaches so far developed to tune and control the molecular porous networks at the surfaces, and our personal perspectives on future challenges and applications of the molecular porous networks.

1. General introduction

Materials science has been an incredibly fascinating and growing field. Thanks to the rapid advancement of nanoscience and nanotechnology, various functional nanomaterials which can be categorized into organic and inorganic systems are becoming highly promising candidates for future nanodevices. Because of their potential applications in electronics [1,2], opto-electronics [2–4], energy storage [5,6], etc., a variety of functional organic nanomaterials have been extensively studied and explored in the past several years [7–11]. Two-dimensional (2D) molecular porous networks (MPNs), which are primarily constructed by organic molecules with various functional groups, represent a family of model systems possessing different types of voids and symmetries that can be further utilized to dock or engraft alien ensembles in the nanofield and to help understand the nature of nanoscience [12].

Like all molecular assembling systems, the final structures of any 2D MPNs are determined by the specific assembling molecules, substrates and environments. Therefore, variations of these three factors would certainly lead to different 2D MPNs.

In three-dimensional (3D) freestanding MPNs, the molecules involved are normally held together by non-covalent interactions such as hydrogen bonding, dipole–dipole interaction, coordination and van der Waals (vdW) force [12]. In contrast, 2D MPNs can hardly be freestanding and have to be supported by a substrate, which in turn adds one more parameter in their driving force, the molecule–substrate interaction. If the 2D MPNs are formed at the liquid–solid interfaces, then a third parameter, namely, the solvent–molecule interaction, comes into play. Ultimately, the 2D porous network structures are the balanced products of various interactions. To design, tune and control the 2D molecular porous network structure involves playing with these balance parameters. Table 1 summarizes the major features of typical non-covalent and covalent interactions.

Among all the molecule–molecule interactions, hydrogen bonds (HBs) have been intensely scrutinized owing to their universal presence and involvement in natural structures, and for their great importance in forming supramolecular systems [13]. However, HBs are known to be fragile to external energy perturbations, thereby stronger but not too strong interactions are needed to construct more complex chemical systems. In this sense, coordination at a surface has emerged as a new approach to tuning 2D MPNs due to its higher stability and directionality compared with other non-covalent interactions [7].

Table 1
A characteristic comparison of several typical non-covalent and covalent interactions.

Interaction type	Interaction energy (kJ mol^{-1})	Directionality
van der Waals force	2–10	No
Hydrogen bonding	5–70	Yes
Coordination interaction	50–200	Yes
Covalent bonding	300	Yes

In studying the 2D MPN structures, scanning tunneling microscope (STM) has proven to be a powerful tool to diagnose the surface structure in real space [7,9,11,14–18]. STM has the flexibility to work under both ultrahigh vacuum (UHV) and ambient conditions. The only limitations for STM are that the substrates must be conducting and their surfaces must not be too lumpy. However, given its atomic and molecular resolutions, it is becoming more and more popular to probe ordered surface structures and even some complicated systems like host–guest complexes [19,20]. To satisfy the surface flatness requirement, organic molecular beam epitaxy (OMBE) is normally employed to deliver stable molecules onto the substrates under UHV conditions and the surface molecule coverage of less than one monolayer can be routinely achieved.

In this review, we present a comprehensive and updated elucidation on tuning and controlling the assembling structures of 2D MPNs. The major concerns are twofold: the internal measures – designs of the molecular building blocks, and the external ones – adjustments of the assembling environments. The efficiency of constructing 2D MPNs is largely determined by the functional groups and the structural geometries of the molecular building blocks. Therefore, careful design of the molecular building blocks is the key to achieving a better self-assembling performance and to devising novel porous networks. Because of their feasibility and utility, most studies focus on the designs of molecular building blocks. In contrast, controlling the 2D MPNs by changing the external factors seems more difficult because the ultimate balance of all the interactions involved for each MPN is actually determined by various environmental elements such as substrate, solvent at liquid/solid interface and the applied bias on electrochemistry scanning tunneling microscope (ECSTM). Accordingly, this review mainly deals with how internal and external measures can be utilized to control and tune 2D MPNs at the surfaces.

2. Internal factors

2.1. Uni-molecular porous networks

Most 2D MPNs reported in the literature are uni-molecular. In this section, we will focus on the uni-molecular systems whose assembling structures are controlled by factors mentioned above, the building block, substrate and assembling environment.

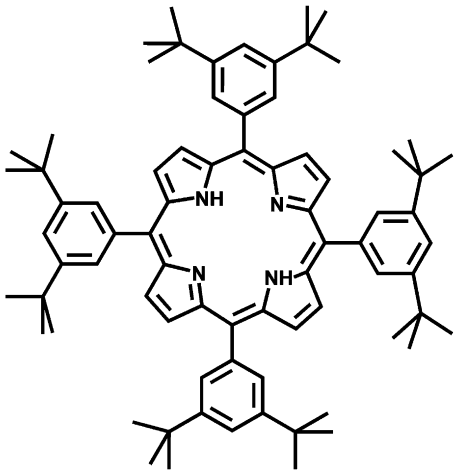

Scheme 1. Molecule structure of H_2-TBPP.

2.1.1. Controlling the building blocks

Upon selecting a proper building block (a single molecule here) for the construction of a 2D MPN, people pay much attention to its functional groups and structural geometry and symmetry. The functional groups determine how strong a molecule interacts with its neighbors in the assembly. Structural geometry and symmetry control the final pattern and symmetry of the assembled 2D MPN. In most cases, the molecule is planar.

An obvious concern in selecting a molecule as a building block is the positions of the functional groups attached. For example, 5,10,15,20-tetrakis-(3,5-di-tertiarybutylphenyl) porphyrin (H_2-TBPP, Scheme 1) and its carboxyphenyl substituted derivatives where one or two *t*-butylphenyl groups in the H_2-TBPP are replaced by carboxyphenyl groups, were employed to study the influence of the structural geometry and symmetry by Yokoyama et al. [21], as shown in Fig. 1. The carboxyl group serves as a typical participant for HB formation, and hence, the positions of the carboxyl groups in the molecule would guide the formation of HBs between neighboring molecules that extend along different directions. Upon adsorption, the *trans*-BCaTBPP and *cis*-BCaTBPP isomers formed conformation-selective assemblies of ordered supramolecular clusters or wires, driven by the optimal coplanar dimerization of the carboxyphenyl groups. Linear *trans*-BCaTBPP self-assembled into supramolecular wires via head-to-head hydrogen bonding (Fig. 1e–h). Due to its two possible chiral conformations upon adsorption, the assembled wire showed a zigzag structure, while the existence of 14.2% defects randomly broke the alternate ordering of the two chiral conformations. *cis*-BCaTBPP, on the other hand, preferentially self-assembled into tetramers at low coverage (Fig. 1i–l). Each conformer of *cis*-BCaTBPP was separated into different supramolecular tetramers, leading to isomeric separation, even though the two *trans*- and *cis*-isomers are nearly energetically identical according to semi-empirical molecular orbital calculations. Similar results were also observed with cyanophenyl substituted H_2-TBPP as a building block for its 2D MPN, where dipole–dipole interaction played a key role in the self-assembly. Its changes in structural geometry allowed structural tuning of the 2D MPNs formed [22]. These experimental results helped prepare supramolecular wires [23,24] and thin films [24]. The lateral nanopores constructed by *trans*-BCaTBPP could act as a secondary host template to accommodate guest molecules like fullerene [25].

Another concern in tuning the pattern and symmetry of the 2D MPNs is the distance from the molecule core to the ending of the attached functional group. This would tune the periodicity and even symmetry of the 2D MPN formed. A series of such studies have been reported by using different assembling molecules containing different molecular cores but the same functional groups. 1,3,5-Benzenetricarboxylic acid (trimesic acid, abbreviated as TMA) is a well-known assembling molecule which forms a whole family of 2D MPNs through its hydrogen bonding either under UHV conditions [26–30] or in solution [31,32]. Its derivatives or analogues were also widely used to construct 2D MPNs [33–35]. TMA molecules can simultaneously form chicken-wire (honeycomb) and flower structures in different domains on highly oriented pyrolytic graphite (HOPG) under UHV conditions [27]. The pore size in both structures is about 1.1 nm, big enough to host some guest molecules including TMA itself. To efficiently use the 2D MPN as a secondary template, it is necessary to control the pore size and inter-pore distance of the 2D MPNs. 1,3,5-Benzenetribenzoic acid (BTB, Fig. 2a), a derivative of TMA by adding a benzyl ring between the original benzyl core and the ending –COOH group of TMA, was used as a building block to construct 2D MPNs on Ag(1 1 1) under UHV conditions (Fig. 2) by Ruben et al. [36] and on HOPG(0 0 0 1) in liquid environment by Lackinger and collaborators [37]. On Ag(1 1 1), the BTB molecules formed a honeycomb structure of 2.9 nm in pore diameter and 3.1 nm in inter-pore distance (Fig. 2), in contrast with the corresponding 1.1 nm (pore size) and 1.7 nm (inter-pore distance) parameters for the TMA honeycomb structure [27]. This is a typical example showing how the 2D MPNs can be tuned by carefully selecting a building block. Ruben et al. [36] also showed that two extra phases could be obtained by annealing the sample to a higher temperature to initiate the deprotonation processes, according to their scanning tunneling spectroscopy (STS) measurements.

A successive and stepwise tuning of the inter-pore distance of the TMA 2D MPNs was realized on Au(1 1 1) under UHV conditions by Ye et al. [29], as shown in Fig. 3. TMA could actually form a series of hexagonal porous networks on Au(1 1 1) under UHV conditions. All structures can be described by a unified model: each half of the rhombus unit cell (bisected by the shorter diagonal) is filled with TMAs in n rows in the form of $1+2+3+\ldots+n$, yielding a total number of $n(n+1)/2$ molecules. The assembling structure is then termed as $H_{TMA\text{-}n}$ for the nth order structure. The TMAs within the half unit cell are held together by trimeric HB and all half unit cells are connected via purely dimeric HB. Obviously, $H_{TMA\text{-}\infty}$ stands for the close-packed assembly as the unit cell length for $H_{TMA\text{-}n}$ approaches infinity and its nanopores disappear. In experiments, structures from $H_{TMA\text{-}1}$ to $H_{TMA\text{-}8}$ and $H_{TMA\text{-}\infty}$, where $H_{TMA\text{-}1}$ and $H_{TMA\text{-}2}$ correspond to the above-mentioned chicken-wire and flower structures, were successfully constructed if the TMA coverage was higher than 0.3 monolayer (ML). In all the observed 2D hexagonal MPNs, the pore size remained about 1.1 nm, whereas the inter-pore distance ranged from 1.6 nm in $H_{TMA\text{-}1}$ to 8.2 nm in $H_{TMA\text{-}8}$ at a step size of 0.93 nm. All the assembled structures are energetically controlled if they are annealed for a long time, and are analyzed in detail in Ref. [29]. Due to the abundant accommodation capability (either via chemical [27] or physical [31,32] interactions) of the pores containing –COOH groups, the precise and stepwise controllability and tunability of the TMA 2D MPNs may have a direct and interesting impact on future studies of host–guest systems.

Similar strategies have also been taken in other systems to extend the knowledge of 2D MPNs. Self-assemblies of three sequentially elongated tetraacid derivatives were compared at a HOPG surface by Zhou et al. [38]. As the assembling molecule elongates along the molecular axis, the assembled 2D MPN pattern changed from a parallel network (Fig. 4a) to a Kagomé structure (Fig. 4b). The two assemblies have nearly identical energies according to DFT calculations, and the intermediate molecule of middle length formed a structure that was a mixture of the other two (Fig. 4c), the short and long ones. A similar phenomenon was also reported by De Feyter and co-workers who chose hexadehydrotribenzo [12]annulene (DBA) derivatives as a model system

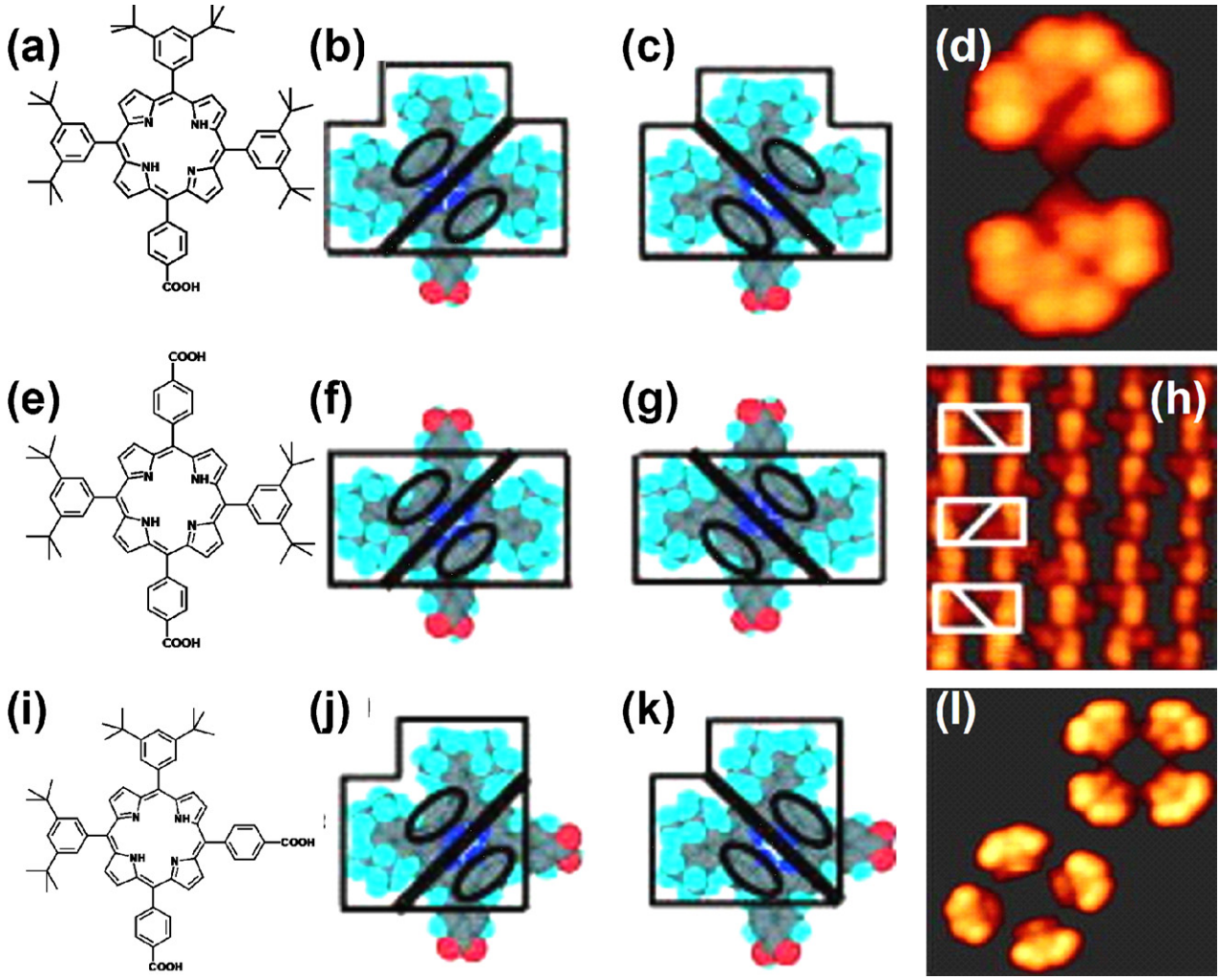

Fig. 1. (a)–(d) CaTBPP structure, its two conformation models and STM image of its dimer consisting of two head-to-head hydrogen-bonded CaTBPP molecules; (e)–(h) *trans*-BCaTBPP structure, its two conformation models and STM image of the zigzag line structure due to its chiral conformations (white frames mark the enantiomers in the assembly); (i)–(l) *cis*-BCaTBPP structure, its two conformation models and STM image of the tetramers constructed via hydrogen bonding between the adjacent two carboxyl groups. All STM images were obtained at 63 K with a negative bias voltage on Au(1 1 1) surface. Reprinted with permission from [21]. ©American Institute of Physics (2006).

to clarify the effects of alkoxyl chain length [39,40], molecular geometry [41] and concentration [42] on the assembly pattern at the 1,2,4-trichlorobenzene (TCB)/HOPG interface. DBA **3a** with six $-OC_{10}H_{21}$ chains (Fig. 5a) formed a honeycomb network, while the other molecules with longer alkoxyl chains such as DBA **3d** and **3e** formed assemblies from linear to complex structures (Fig. 5b). The structural transformation from the honeycomb to the linear structure was a compromise of different interactions such as the molecule–molecule, molecule–substrate and molecule–solvent interactions. This proposition was supported by the fact that co-adsorption of some big planar π-conjugated guest molecules helped to build a honeycomb structure [39] in the DBA systems, and other selected guest molecules helped form other assembling structures [43]. Unfortunately, the compromise of these interactions that ultimately determine the structures of 2D MPNs is hardly predictable, especially at the liquid/solid interfaces.

Elongations along the molecular axes of the assembling molecules have generated a series of similar studies in the past years, which aimed at obtaining well controllable 2D MPNs, mainly focusing on the effects of the alkyl chains [44–48] and molecular size [49–52]. Such studies are becoming more and more attractive due to the requirement of precise control and tuning of the 2D MPNs that may serve as secondary templates. It is widely believed that this strategy should help turn the self-assembling process into an efficient and applicable bottom-up approach to fabricating large-area nanostructures at a surface.

At the same time, people are also making great efforts to construct and control 2D chiral architectures, especially the chiral MPNs, from achiral or prochiral precursors. As the architecture dimension lowers from 3D to 2D, its chirality could randomly emerge. Very recently, Xiao et al. [53] reported the fabrication of a 2D chiral MPN. They used 1,3,5-tris(4′-carboxyphenyl)-2,4,6-tris(4′-*tert*-butylphenyl)-benzene (Fig. 6a and b) as the building block to successfully construct honeycomb structures (Fig. 6c) on Au(1 1 1). A family of 2D MPNs were prepared, named as HC_1 to HC_4 (Fig. 6d–g) where the number stands for the number of molecules per unit cell length, similar to the terminology for the TMA system [29]. This reported assembling system differs from the TMA one in two aspects: (a) the two half unit cells for the assembling structures from HC_2 through HC_4 display opposite handedness, and the whole structure is racemic; (b) in assembling structures from HC_2 to HC_4, all building molecules are connected by vdW force in the unit cell, in contrast with HBs in the TMA structures. The introduction of chirality in the work by Xiao et al. [53] was dependent on the dihedral angle caused by the rotation of the σ-bond connecting the central benzene core and the external phenyl ring. Prior to this report, 2D chiral MPNs were actually achieved with other building blocks [54–59], but none of them could simultaneously control the

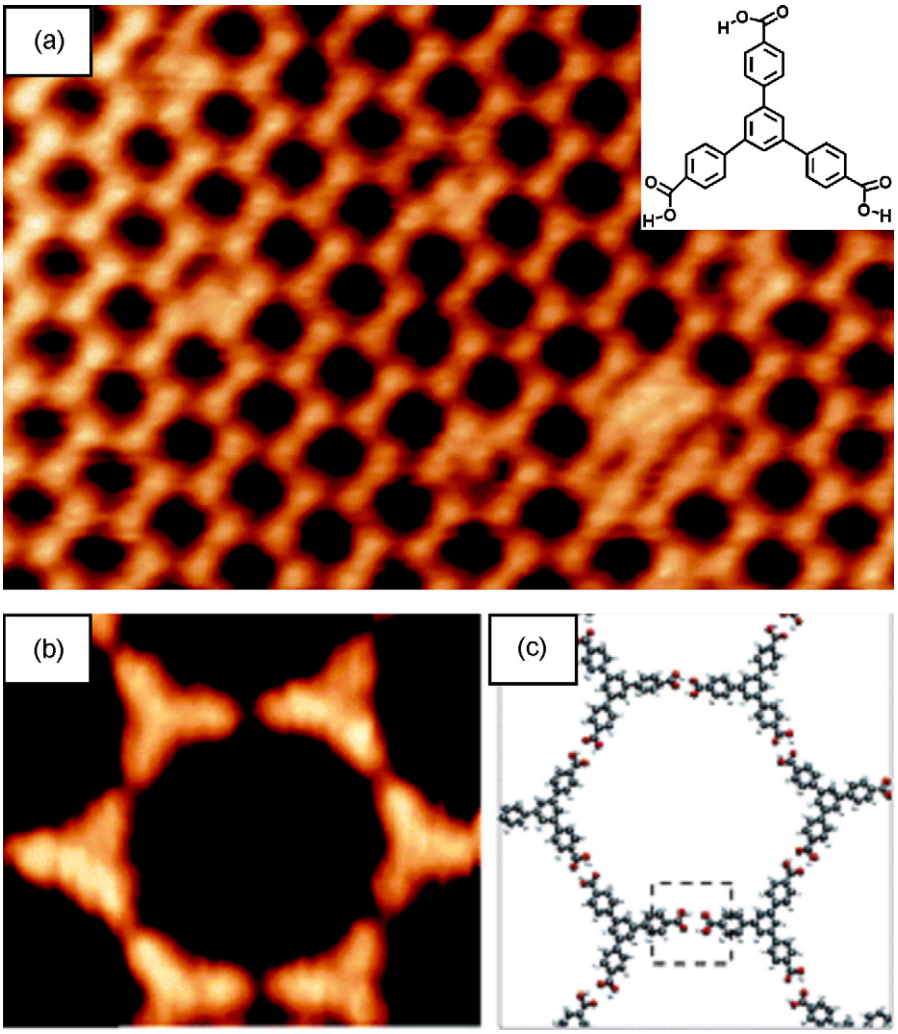

Fig. 2. (a) STM image of an ordered chicken-wire network formed by deposition of BTB on Ag(1 1 1), 30 nm × 20 nm (inset is the molecular structure of BTB); (b) an enlarged STM image of a hexagonal pore in the assembly, 4.9 nm × 4.3 nm and (c) molecular model for the hexagonal pore. Reprinted with permission from [36]. ©American Chemical Society (2006).

chirality and structural parameters of the 2D MPNs. According to Schlickum et al. [60], a similar chiral MPN can also be realized by changing the chain length along the molecular axis.

Using a building block with a cavity inside is another strategy to construct 2D MPNs. Porphyrin, phthalocyanine and their derivatives are popular molecules used in surface assemblies because of their planar structures and unique physicochemical properties suitable for wide applications in photochemistry, electronics, catalysis and solar cells [61–66]. The 2D MPNs constructed by porphyrins have been reviewed recently [19,20], and here we focus on other building blocks with a cavity inside. Wan and co-workers [67–69] have carried out a series of studies on the self-assembly of calixarenes using ECSTM. In contrast to the pores constructed by cross-linking of the building blocks, calixarenes already possess internal pores whose sizes can be tuned by simply changing the molecular backbones. Moreover, the resulting patterns can be drastically influenced by the external functional groups. Each calix [8]arene incorporated with a fullerene molecule can feasibly assemble at a surface [67]. Self-assemblies of cyclothiophenes can accommodate fullerene molecules due to their relatively stronger interactions with fullerenes [70–73]. Recently, Panet al. [71] reported that a special macrocycle molecule with a bithiophene unit (see the molecular structure in Fig. 7) self-assembled to form two types of pores on HOPG at the liquid/solid interface (Fig. 7a–c). STM measurements showed that an intrinsic pore **A** in the core was about 1.4 nm in diameter, and pore **B** which was surrounded by the distorted alkyl chains and the molecular core was about 2.5 nm × 1.8 nm (Fig. 7c). Fullerene molecules preferred sitting atop the bithiophene groups rather than in pore **A** or **B** because the interaction of fullerene and thiophene groups is stronger than that of fullerene and the HOPG substrate. Such a network with two different pores can also be constructed by a porphyrin derivative [19] and is able to host two guest molecules simultaneously.

2.1.2. *Tuning the inter-molecule interactions*

As stated before, inter-molecule interactions play a significant role in holding the assembled molecules together to form 2D MPNs. In self-assemblies, these inter-molecule interactions are typically non-covalent, including hydrogen bonding, vdW force, metal–ligand coordination, dipole–dipole interaction, electrostatic interaction and so on. 3D supramolecular architectures mainly rely on these non-covalent interactions [74–76] that also apply for 2D self-assemblies and MPNs [12]. According to previous studies [7,77,78], these interactions can drastically vary in strength and cause great differences in their stability and directionality as shown in Table 1. The vdW force universally exists in nearly all 2D MPNs, but is normally too weak to resist external energy perturbations, leading to poor stability of the 2D MPNs formed. Hydrogen bond-

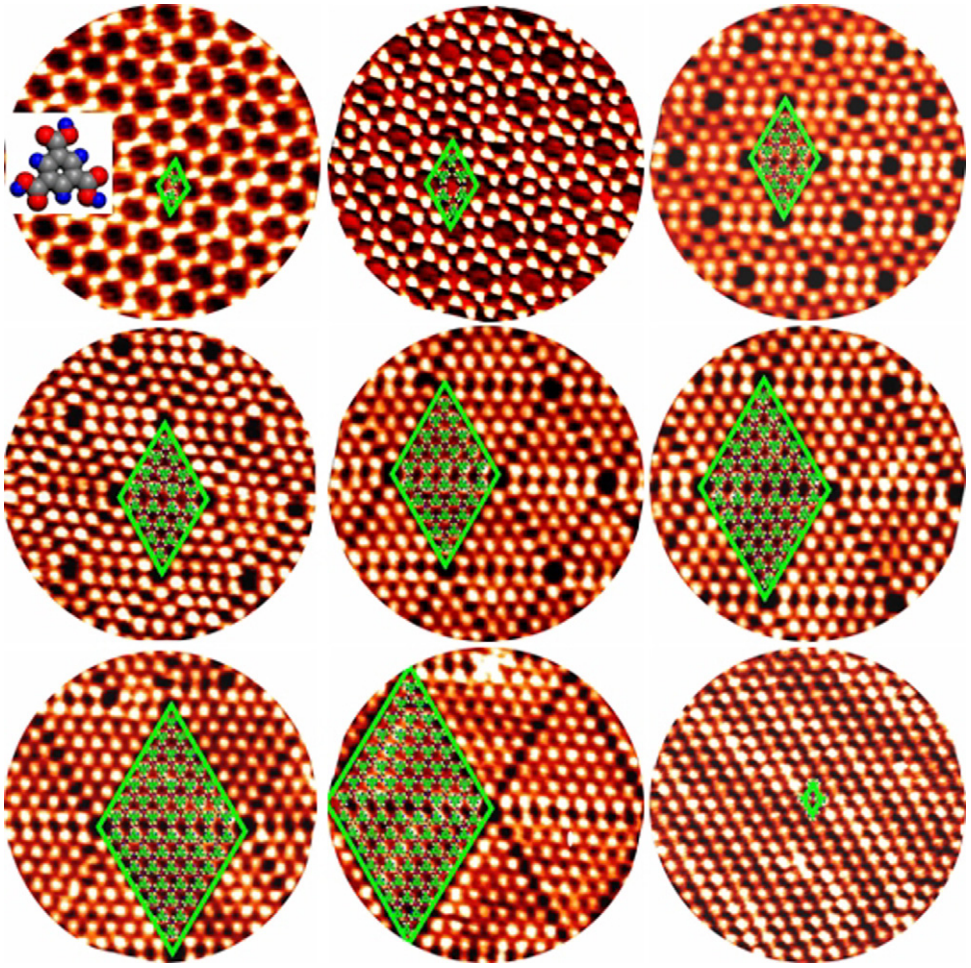

Fig. 3. A series of STM images of the 2D MPNs formed by TMA on Au(1 1 1). Starting from the chicken-wire structure (top-left, with a TMA molecule model inserted) to the close-packed one (bottom-right), the inter-pore distance is increased at a step size of 0.93 nm. All structures are named as from $H_{TMA\text{-}1}$ through $H_{TMA\text{-}8}$ and $H_{TMA\text{-}\infty}$, as stated in the context. In each image, the unit cell is marked. The results have been reported in [29].

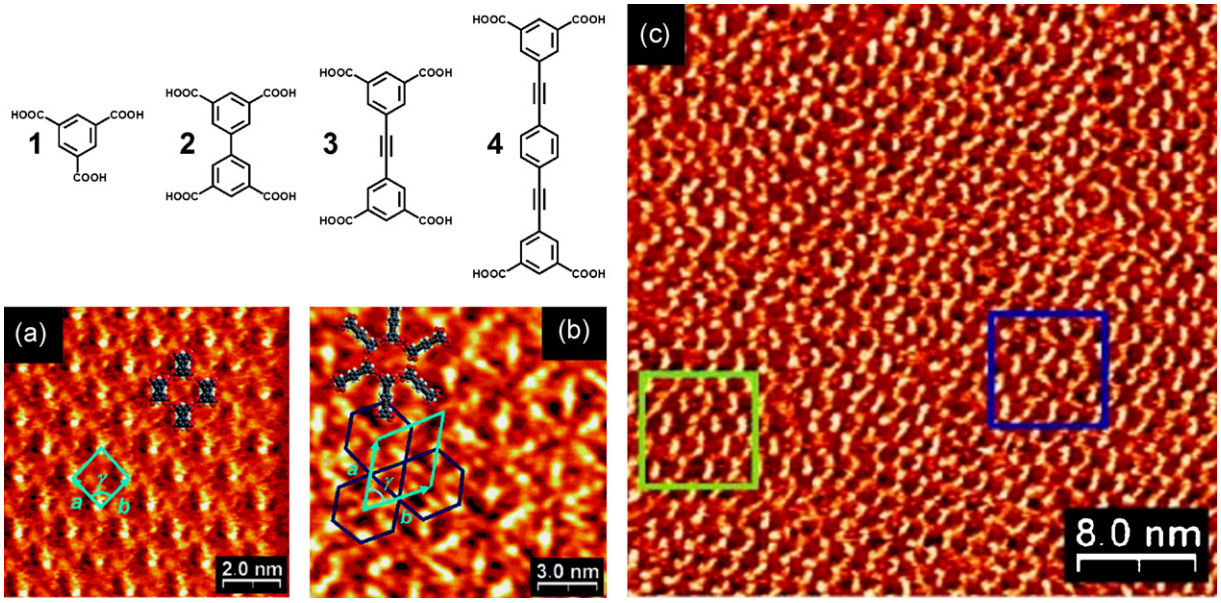

Fig. 4. Molecular models for TMA (**1**) and its three analogues named as **2**, **3** and **4**. (a) and (b) STM images of a parallel network formed by molecule **2** and a Kagomé structure formed by molecule **4** (light blue frames and dark blue pattern correspondingly mark the unit cells and the Kagomé network, and molecular models are superimposed for visual assistance); (c) STM image showing the assembling structure by molecule **3**, combining both structures in (a) and (b) (green and blue frames indicate regions for the parallel network and Kagomé network, respectively). Adapted from [38].

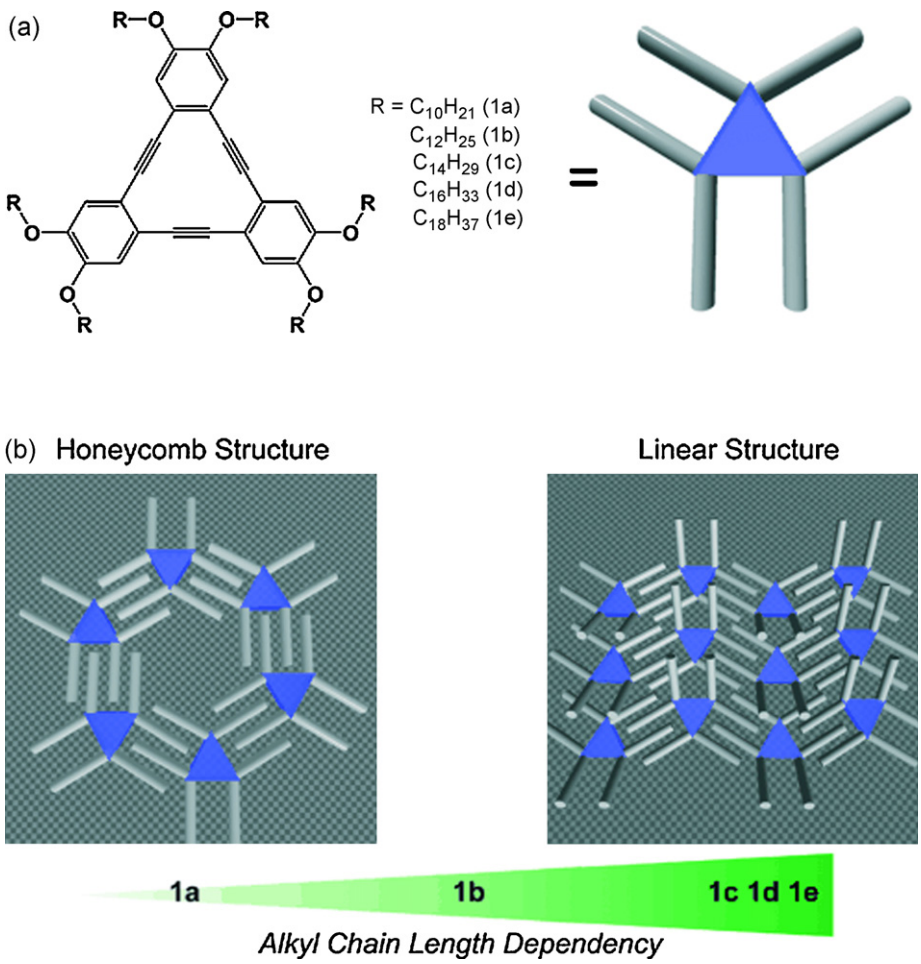

Fig. 5. (a) Schemes illustrating DBA derivatives with different alkyl chains and (b) molecular models showing the transformation from honeycomb to a linear formed structure as a function of the attached alkyl chain length. Reprinted with permission from [39]. ©John-Wiley (2007).

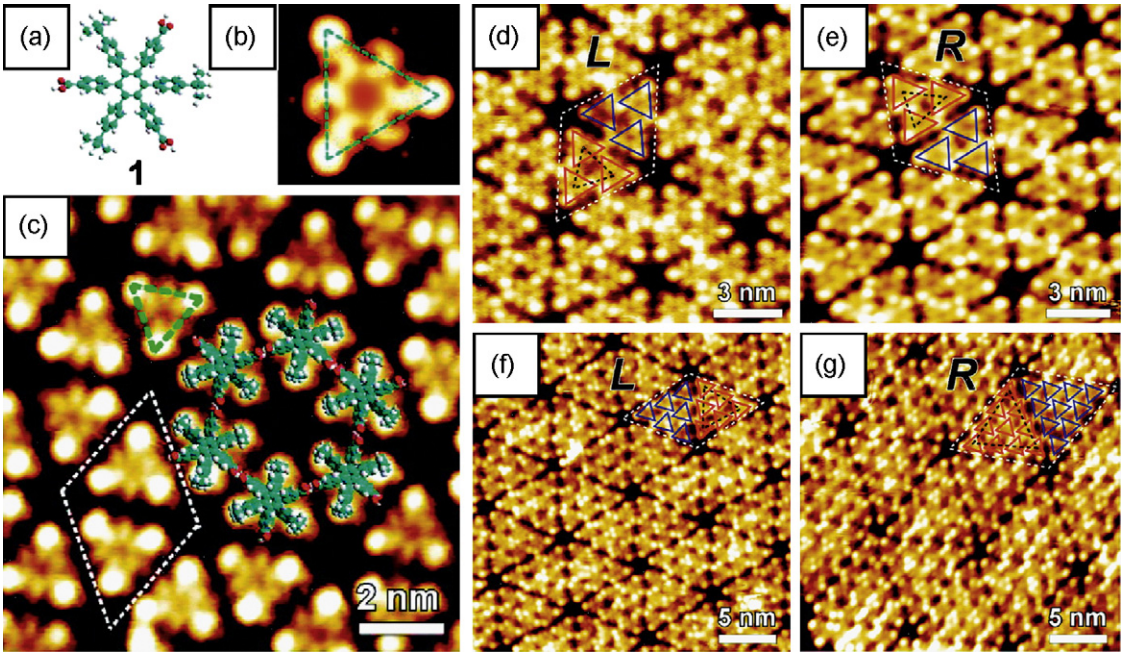

Fig. 6. (a) Molecular model of the building block, 1,3,5-tris(4′-carboxyphenyl)-2,4,6-tris(4′-*tert*-butylphenyl)-benzene; (b) theoretically simulated STM image of the molecule; (c) the honeycomb structure of HC_1 without chirality; (d) and (e) L- and R-domains of the HC_2 structure; (f) L-domain of the HC_3 structure; (g) R-domain of the HC_4 structure. Unit cells are indicated by white dashed lines. Individual molecules are highlighted as red and blue triangles (opposite chiral conformations of the molecules) with corners at *tert*-butyl positions. Reprinted with permission from [53]. ©American Chemical Society (2008).

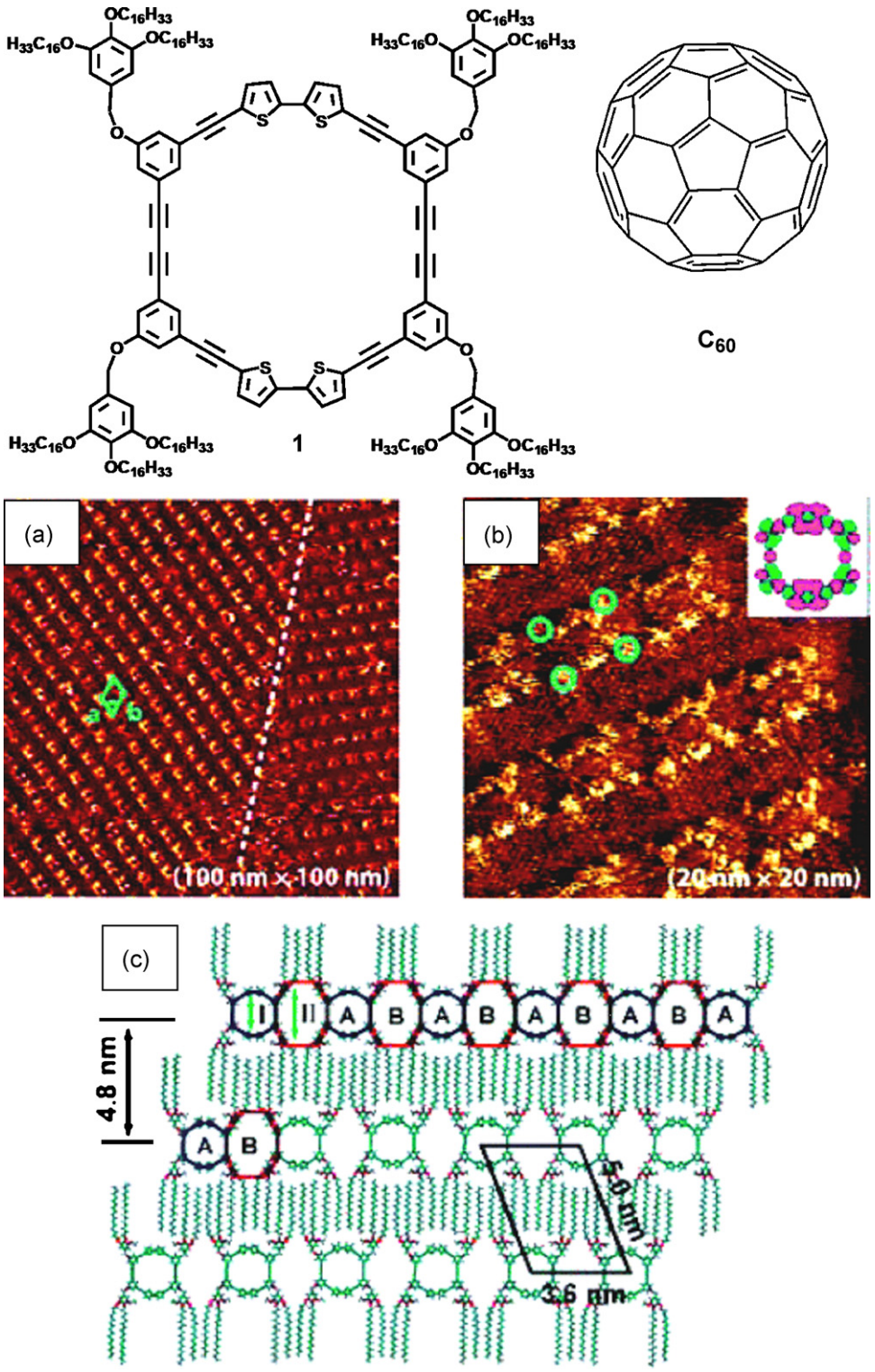

Fig. 7. The specific self-assembled porous structure of the chosen macrocycle molecule (**1**). (a) Large-area STM image with two domains separated by the dash line (unit cell highlighted in green); (b) high-resolution STM image (green circles marking the four extraannular groups, and the inset being the HOMO of the cyclic backbone of molecule **1**); (c) the proposed structural model. Two types of pores, namely, A and B, are shown in the proposed model. C_{60} was used as a guest to study the accommodation behavior of this system. Reprinted with permission from [71]. ©American Chemical Society (2006).

ing, however, is widely used to construct 2D MPNs because of its directionality and relative stability [78]. Similarly, metal–ligand coordination is also widely employed, especially under UHV conditions, because it is much more stable than other interactions in terms of bonding energy. Needless to say, 2D MPNs can also be formed by covalent bonds [79] that overtake non-covalent ones and hence, possess a much higher thermal stability. However, the more stable the 2D MPNs based on the covalent bonds, the more difficult to tune them. Thus, people prefer to utilize non-covalent interactions like vdW forces, hydrogen bonding and metal–ligand coordination to construct 2D MPNs. Herein, we present a series of examples showing the importance and necessity of choosing a

suitable inter-molecule interaction to construct, tune and control the structures of 2D MPNs.

2.1.2.1. Hydrogen bonding. In a typical donor–acceptor system [80–82], hydrogen bonding mainly works via the terminal functional groups in the assembling molecules, including –COOH, –OH, $–NH_x$ ($x \geq 1$) and so on. Due to their suitable bonding strength, several exciting 2D MPNs with excellent tunability, controllability, predictability and foreseeable applicability have been realized [29,53]. Since Cicoira et al. have already given an excellent review on this [12], we only briefly mention some other systems here.

As described before, TMA [26–32] is a well-documented molecule that elegantly makes use of hydrogen bonding to construct 2D MPNs in a well controlled manner. Stöhr et al. [83] showed that 9-diaminoperylene-quinone-3,10-diimine (DPDI, Fig. 8a) could form a 2D MPN structure at a coverage of 0.1–0.7 ML on Cu(1 1 1) (Fig. 8b) under UHV conditions. It is believed that the highly stable hexagonal porous structure was constructed by the HBs between deprotonated amino groups. An increase in coverage would lead to a close-packed structure, eliminating the pores. The same group of scientists also studied in detail the accommodation behavior of zinc octaethylporphyrin (ZnOEP) and fullerene on the DPDI MPN, as shown in Fig. 8c [84].

2.1.2.2. Metal–ligand coordination. In contrast to the hydrogen bonding system, Kern and co-workers [85] first reported in 2002 the construction of 2D MPNs by using metal–ligand coordination (a coordination system being a multiple-body one, involving at least two components—the metal core and organic ligand, we here only stress the role of the ligand). In that report, deprotonated TMA molecules coordinated with Cu adatoms evaporated from the kinks or step edges on Cu(1 0 0). In accordance with the coordination number of Cu^{II} in bulk materials, a fourfold coordination complex of $[Cu^{II}(TMA)_4]^{n-}$ was formed. Within a couple of years after the Kern group's report, several groups also constructed various types of coordinated 2D MPNs at the surfaces with metal atoms like Fe [50,56,86–91], Co [51,52,88], Mn [92,93] and Cu [87]. Both experimental results [94] and theoretical calculations [95] confirmed the formation of the surface bound metal–ligand complexes.

The ultimate geometry of a coordinated 2D MPN depends strongly on the coordination number, as pointed out by Lin and co-workers [88]. The coordination complexes of 4,4′-biphenol ligand (**1**, Fig. 9a) with Fe ions (Fig. 9b and c) and 1,4′,4′,1″-terphenyl-4,4″-dicarbonitrile ligand (**2**, Fig. 9d) with Co ions (Fig. 9e) were successfully prepared on site at a surface, forming 2D hexagonal MPNs. A threefold porous coordination network constructed by Fe ions and ligand **1** was not found in the 3D bulk materials, nor was it formed by Co ions and ligand **2**. With the dimensional restrictions at the surface, such unusual threefold MPNs could only be prepared under UHV conditions. In contrast to the appearance of chirality in the Fe-**1** network on Ag(1 1 1) (Fig. 9b) and Cu(1 0 0) (Fig. 9c), Co–**2** network displayed a typical hexagonal structure on Ag(1 1 1) (Fig. 9e). Furthermore, Lin et al. also studied the influence of the substrate by using Ag(1 1 1) and Cu(1 0 0) which have different surface symmetries. One of the two MPNs constructed by Fe-centered coordination complex on Ag(1 1 1) was replaced by two novel ones on Cu(1 0 0).

Unlike the unusual aforementioned hexagonal MPNs, most 2D MPNs reported in the literature possess fourfold symmetry. The carboxyl group is one of the most frequently used ligand and Fe usually serves as a metal core that has a high chemical reactivity. Tuning and control of such coordinated 2D MPNs heavily rely on the structural geometries of the coordinated building blocks [50,96] and the relative ratio of metal to ligand [90,94], respectively. For example, terephthalic acid (TPA) could be used as the ligand coordinating to an Fe ion on Cu(1 0 0) [90]. When the Fe/TPA ratio became 0.3:1 (panel A in Fig. 10), 0.8:1 (panel B in Fig. 10) and 1.2:1 (panel C in Fig. 10), several 2D MPNs were formed at the surface and named as "cloverleaf phase" (Figs. a–c in panel A, Fig. 10), "ladder phase" (Figs. a and b in panel B, Fig. 10) and "single-row phase" (Figs. a–c in panel C, Fig. 10), respectively. Since these structural transformations underwent thermal treatments at relatively high temperatures, these 2D MPNs were thermally stable, making them plausible as stable secondary templates.

2.1.2.3. Chemical bonding. Covalent chemical bonding as a new strategy to construct 2D MPNs at the surface was recently reported [79]. It differs from the traditional non-covalent interactions only in the bond strength. As the building blocks are held together by chemical bonds, the 2D MPNs so produced are superior in thermal stability to those formed by non-covalent interactions. On Ag(1 1 1), Zwaneveld et al. [97] successfully prepared 2D MPNs through the dehydration reaction of 1,4-benzenediboronic acid (BDBA, panel A in Fig. 11) or BDBA with 2,3,6,7,10,11-hexahydroxytriphenylene (HHTP, panel B in Fig. 11) under UHV conditions. Both dehydration reactions occurred at or below room temperature and did not need extra manipulation with an STM tip or further annealing, inferring the existence of a very low energy barrier for such reactions. Well ordered 2D MPNs at a surface coverage ranging from less than 1% up to almost 100% were routinely obtained by controlling either the temperature of the evaporator and substrate or subsequent annealing temperature. The prepared 2D MPNs could be stable up to 750 K, which greatly extends their applicability as secondary porous templates.

The chemical bonding strategy has flourished in recent years, in preparing novel 2D MPNs [98–101], demonstrating its availability and diversity in constructing 2D MPNs based on a variety of surface chemical reactions. Metallic surfaces are extensively used, possibly due to their catalytic activity. Metals have two advantages: on the one hand, some unfavorable reactions under ambient conditions may be initiated at the surface under UHV conditions; on the other hand, conventional and powerful surface analysis techniques such as STM, X-ray photoelectron spectroscopy (XPS), low energy electron diffraction (LEED), etc. offer scientists many opportunities to scrutinize the network structures and explore the mechanisms of surface chemical reactions. Apparently, the 2D MPNs prepared by surface chemical reactions can be used as stable secondary templates to host foreign molecules or clusters and even as microcavity reactors. However, the chemical stability makes it extremely difficult to tune and control the 2D MPNs afterwards. Therefore, one has to carefully choose the reactants and reactions from the very beginning in order to control the structures of the 2D MPNs.

In general, a direct comparison of various interactions among different building blocks is not likely possible and straightforward because their working mechanisms and interaction strengths are usually different. Nevertheless, exploring and understanding the inter-molecule interactions can obviously bring about abundant information and knowledge that can in turn guide our building, design and tuning of 2D MPNs.

2.2. Bi-molecular porous networks

2D MPNs constructed by binary or multiple components are drawing more and more attention because there exist more flexibilities to design and prepare more complex 2D porous structures and more subtle ways to tune and control the assembling structures. With the add-in of a second assembling molecule, the original balance of the interactions in the uni-molecular systems is broken or shifted. If the original balance is completely broken, the original assembling structure will break down; if the original balance is shifted, then a new assembling structure will appear. The latter will certainly offer new chances to construct new 2D MPNs.

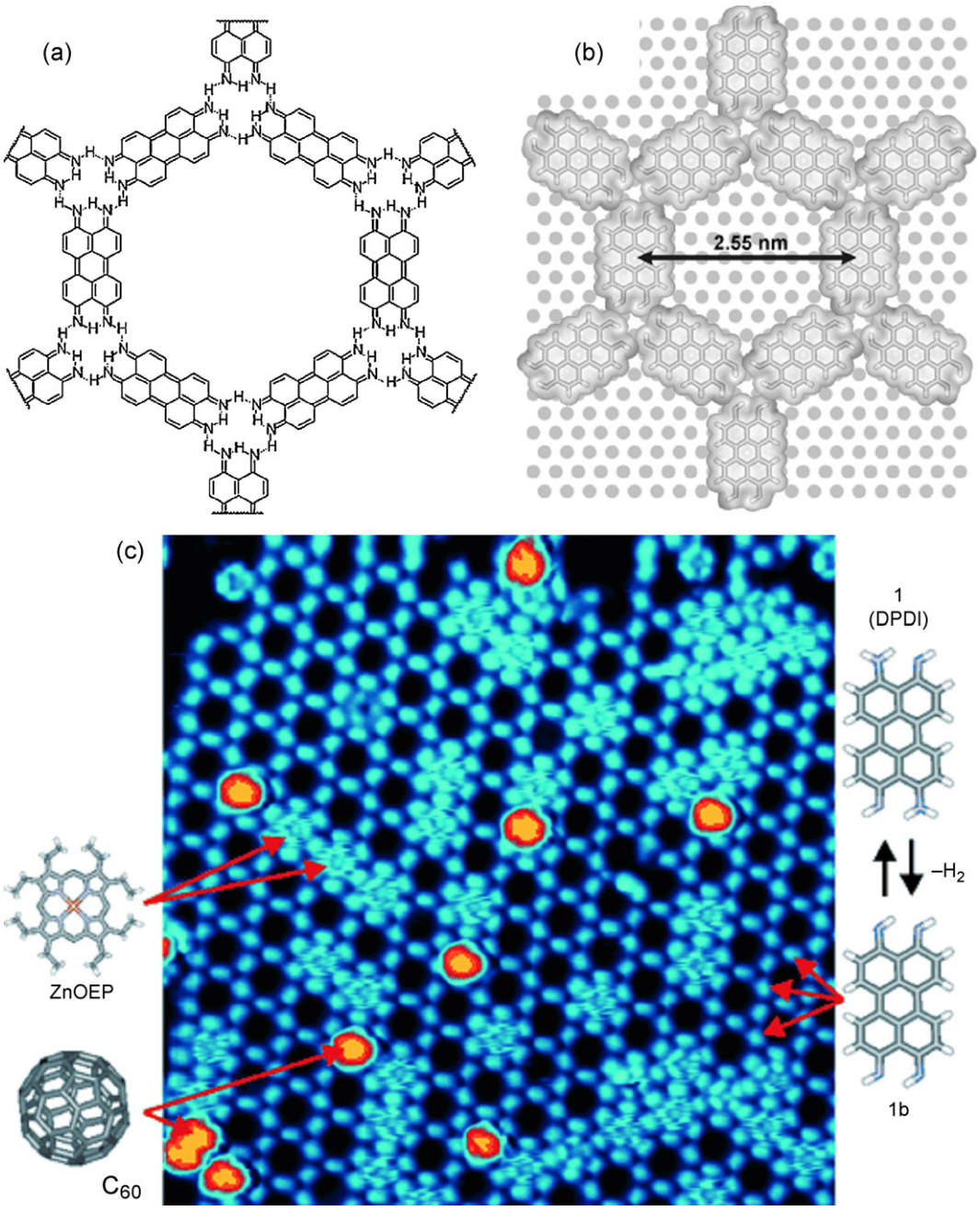

Fig. 8. (a) and (b) Chemical structure and assembled porous network model of the dehydrogenated DPDI plus the Cu(1 1 1) lattice; (c) STM image of the hexagonal porous network hosting ZnOEP and C_{60}, 30 nm × 30 nm. The arrows indicate the corresponding chemical structures assigned to the molecular units. Reprinted with permission from [84]. ©John-Wiley (2007).

In the uni-molecular systems, there are only three interactions, namely, inter-molecule, molecule–substrate and molecule–solvent interactions. In binary systems, there appear several more interactions: molecule 1–molecule 2, molecule 2–molecule 2, molecule 2–substrate and molecule 2–solvent interactions. All these additional interactions add more difficulties in controlling the 2D MPNs, yet bring more parameters to tune the 2D MPNs. This is the reason that people are adopting the binary system to construct novel 2D MPNs. As a matter of fact, a similar strategy has already been used in traditional surface science studies in the past decades to tune co-adsorption structures at the surface. For example, co-adsorption of benzene and CO on transition metal substrates normally yields a better ordering of the coadsorbates [102]. Admittedly, selecting the second component is very challenging because frequently it could cause clustering at the surface and each type of assembling molecules may self-assemble into separate domains.

So far, we unfortunately do not have a general guiding theory at hand that allows us to precisely introduce the second component without messing up the original uni-molecular 2D MPNs. Empirically, we could obey the following ambiguous, yet useful, rules: (a) If the adsorptions of two coadsorbing molecules can change the work function of the substrate in opposite ways, they would stabilize each other and hence, their assembling would be strengthened at the surface. (b) If the interaction strengths of both molecules with the solvent are competitive, but not too strong, there exists a higher possibility to achieve better ordering of the binary system at the surface.

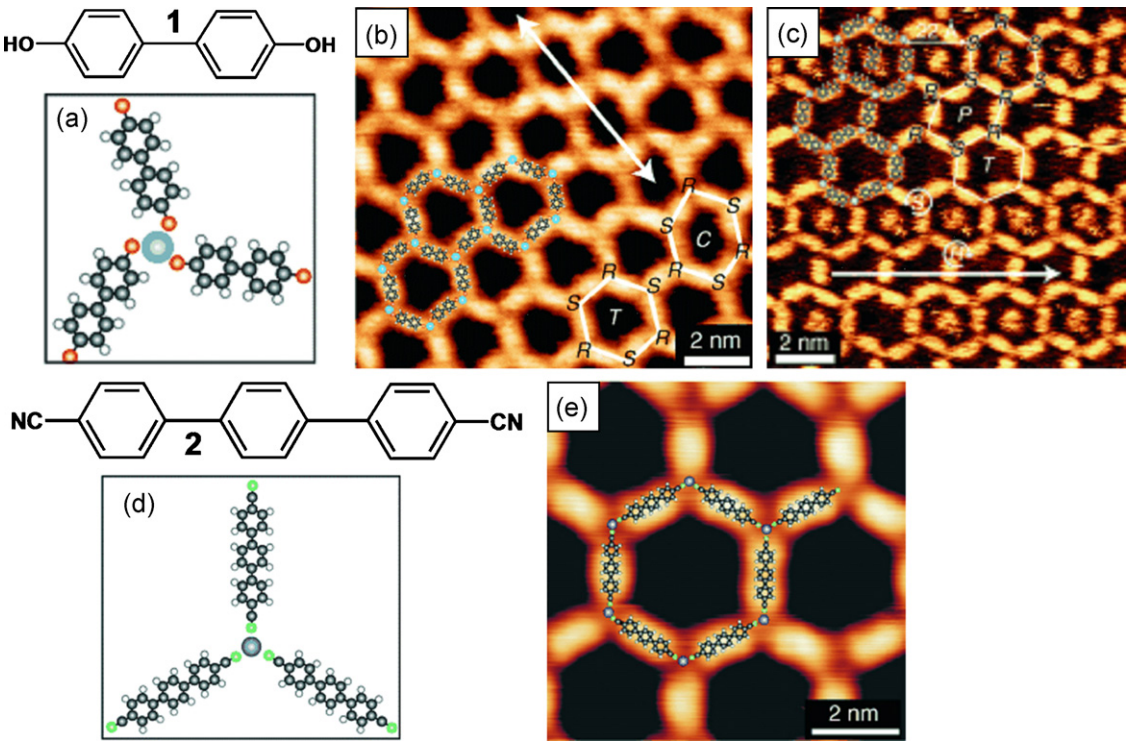

Fig. 9. (a) Schematic drawing of molecule **1** coordinated to Fe; (b) the Fe-**1** coordinated porous network with two types of pores, T and C, on Ag(1 1 1); (c) the assembled Fe-**1** network on Cu(1 0 0), consisting of three types of pores, namely, P, F and T; (d) schematic model of molecule **2** coordinated to Co and (e) STM image of the Co–**2** assembly with a highly symmetric hexagonal pore on Ag(1 1 1). Colors: C gray; H white; O red; N green; Fe light blue; Co dark blue. Adapted from [88]. ©John-Wiley (2007).

Fortunately, people have successfully prepared some intriguing bi-molecular 2D MPNs. We here summarize these 2D MPN systems, following the categories in above sections.

2.2.1. Controlling the building blocks

Once again, selections of different building blocks will absolutely lead to different 2D MPNs because the inter-molecule interactions and the structural geometries as well are changing simultaneously. Although different types of 2D MPNs have been reported, few researchers have discussed in detail why they could tune and control the assembling structures of the 2D MPNs. A successful study was accomplished by Langner et al. [103] on Cu(1 0 0), as displayed in Fig. 12. According to their previous experiments [104], linear polyaromatic bipyridine molecules could coordinate to Cu adatoms to form chain-like structures that were randomly distributed at the surface. In Ref. [103], the authors adopted two linear polyaromatic bipyridine molecules of different length as the organic ligands (P1 and P2) and two linear bis(carboxylic acid) molecules as the connectors (C1 and C2) of the coordinated chains in parallel. As shown in Fig. 12, different combinations of the ligands and

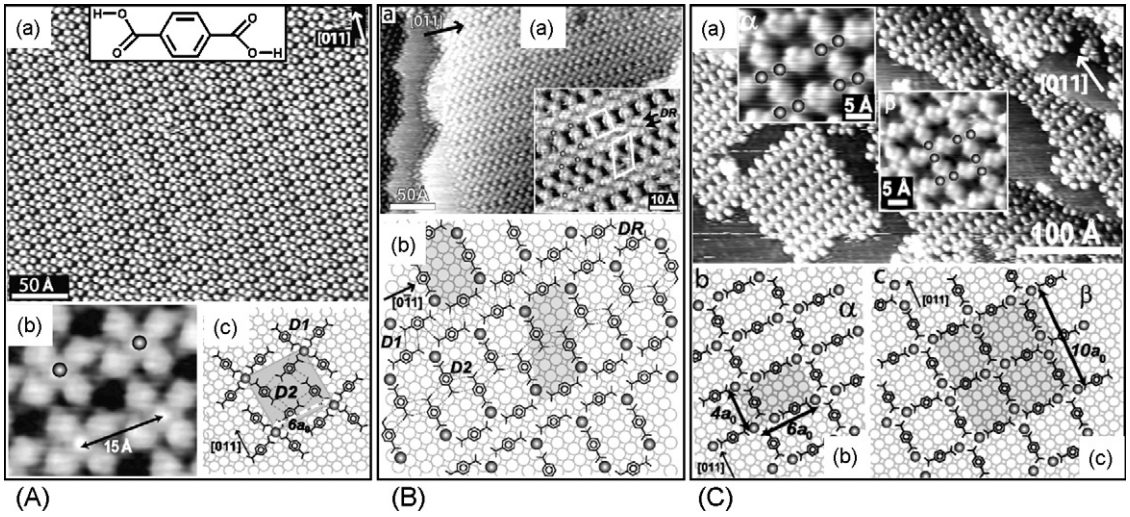

Fig. 10. Panel A, Fe–TPA coordination structure at an Fe:TPA ratio of 0.3:1, named as "cloverleaf phase". (a) and (b) Large-area and high-resolution STM images; (c) schematic drawing of the assembly (potential C–H···O hydrogen bonds are indicated, and the O···H–C distance $D_1 = D_2 = 3.5$ Å). Panel B, Fe–TPA coordination structure at an Fe:PA ratio of 0.8:1, named as "ladder phase". (a) Large-area STM image with a high-resolution image inserted and (b) schematic drawing of the assembly (the O···H–C distance is 3.0 Å). Panel C, Fe–TPA coordination structure at an Fe:TPA ratio of 1.2:1, named as "single-row phase". (a) STM images of two types of the assembling structures, each with a high-resolution STM image inserted; (b) and (c) corresponding structural models. Adapted from [90]. ©John-Wiley (2004).

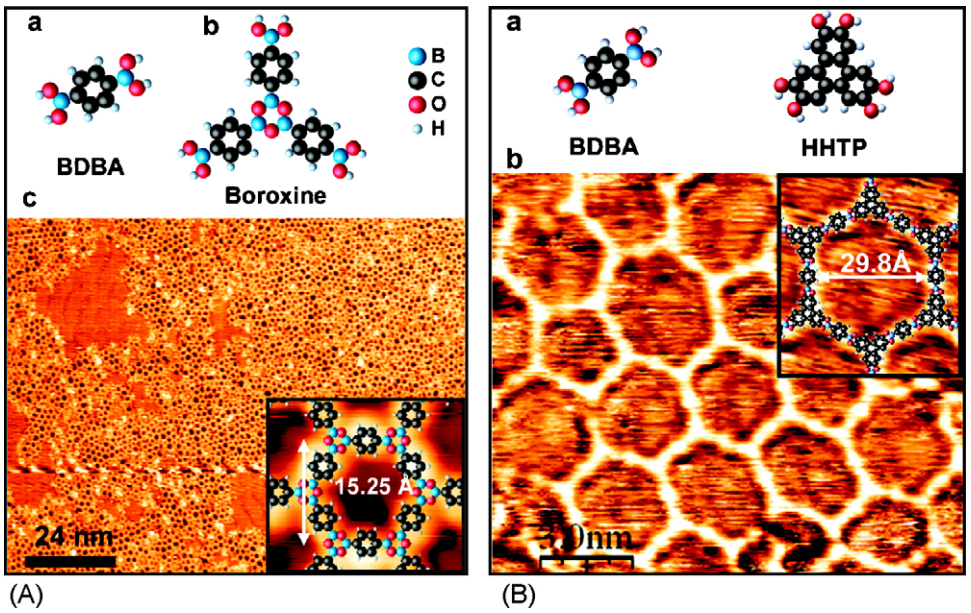

Fig. 11. Panel A, (a) chemical structure of the reactant BDBA; (b) the repeat unit of the product Boroxine; (c) large-area STM image of the nearly monolayer product on Ag(1 1 1) with theoretically calculated STM image inserted. Panel B, (a) chemical structures of the reactants BDBA and HHTP; (b) STM image of resulted porous structure on Ag(1 1 1) with modeled molecules superimposed. Reprinted with permission from [97]. ©American Chemical Society (2008).

connectors yielded different assembled structures. The connectors greatly enhanced the thermal stability of the coordinated chains via hydrogen bonding, indicating that hierarchical interactions consisting of metal–ligand coordination and hydrogen bonding were established in the same system. Accurate controllability was therefore achieved by controlling the molecular lengths of the ligand and the connector. Combination of three different ligands was also applied to study the self-selection phenomenon of this system [105].

The above example clearly demonstrates the feasibility and capability of tuning and controlling 2D MPNs constructed with binary components. Such binary systems usually yield different patterns based on the changes caused by either of the binary components, which seems more attractive and flexible to construct 2D tunable MPNs than the uni-molecular systems. However, in reality, only a few studies actually accomplish this tuning because of the complexity of the binary systems. Thus, a deep and thorough understanding of such systems awaits more experimental results in the future.

2.2.2. Tuning the inter-molecular interactions

2.2.2.1. Hydrogen bonding. In a uni-molecular system, only the inter-molecule interaction between the same assembling molecules is involved. In bi-molecular systems, two additional inter-molecular interactions, molecule 1–molecule 2 and molecule 2–molecule 2, would increase the complexities. These multiple interactions can be termed as hierarchical interactions, as stated in report mentioned above [103]. In the literature, a majority of

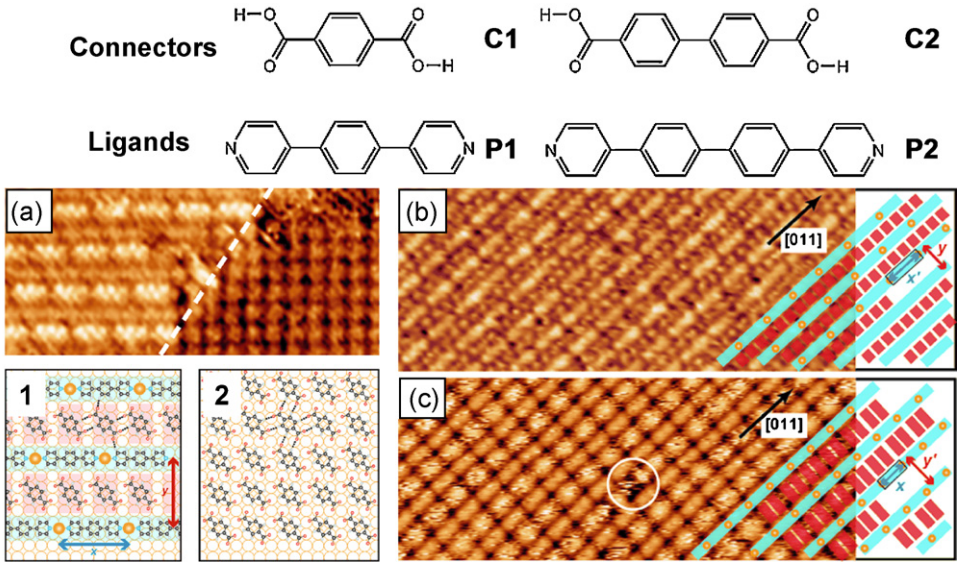

Fig. 12. Structural models of the connectors C1 and C2, and ligands P1 and P2. (a) High-resolution STM image of the P1/C1 hierarchical assembly domain (model **1**) and the C1 hydrogen-bonded network domain (model **2**), 140 Å × 63 Å; (b) and (c) STM images of the P2/C1 and P1/C2 hierarchical assembling structures, 25 nm × 10 nm. The circle marks the missing C2 defect. The brick-like schematic models show the tuning of the network parameters *x* and *y* (to *x* and *y*') by replacement of the connector C1 with C2. Adapted from [103]. ©John-Wiley (2008).

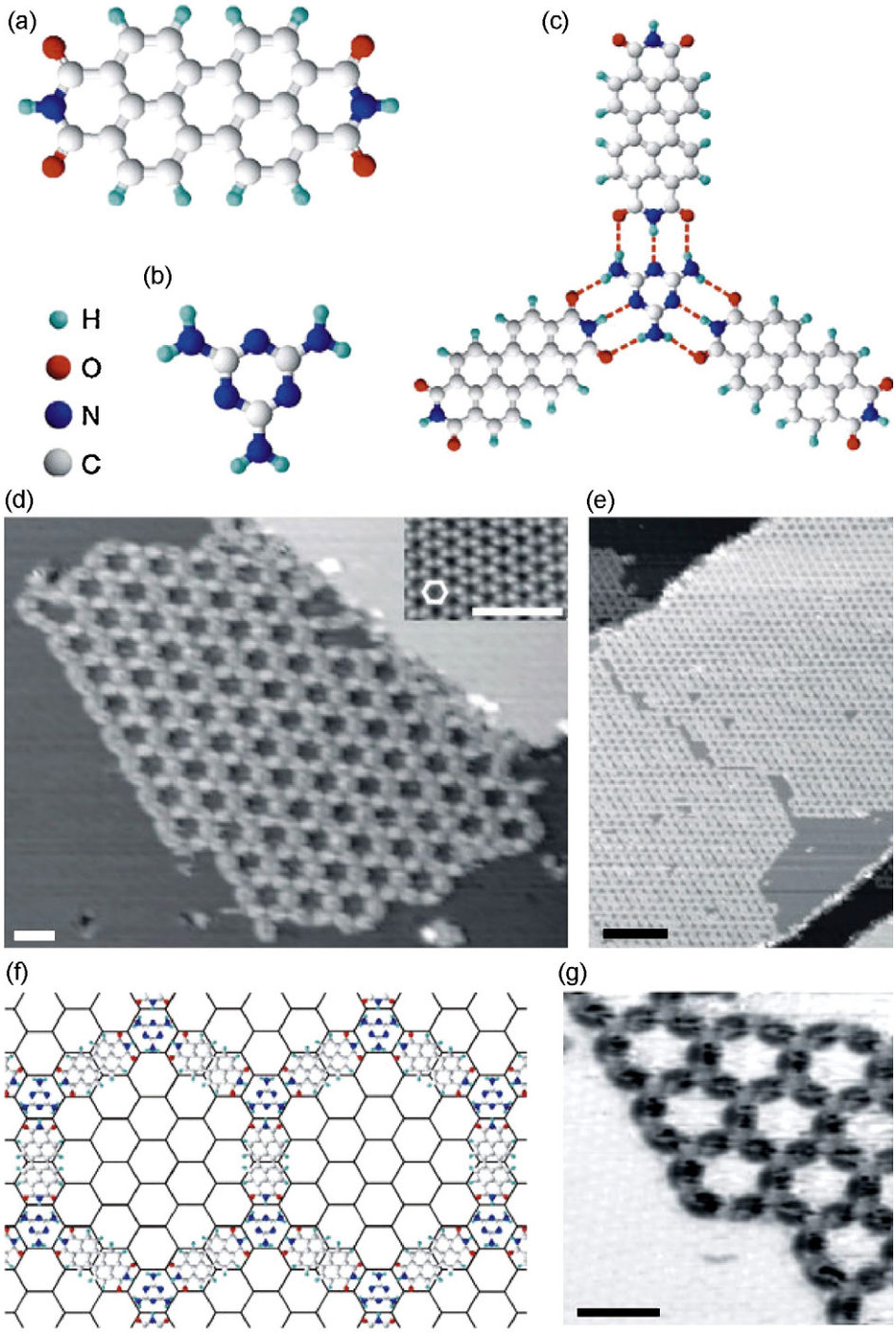

Fig. 13. Chemical structures of (a) PTCDI and (b) melamine; (c) the repeat unit of the assembling structure; (d) STM image of the PTCDI-melamine assembly showing the highly symmetric hexagonal porous network. The inset is a high-resolution STM image of the substrate, Si(1 1 1)-($\sqrt{3} \times \sqrt{3}$)-R30°-Ag. Scale bars, 3 nm; (e) the self-assembled network extending across steps. Scale bar, 20 nm; (f) structural model of the hexagonal network and (g) an inverse contrast STM image. Scale bar, 3 nm. Reprinted with permission from [106]. ©Nature Publishing Group (2003).

studies on bi-molecular systems focus on constructing 2D MPNs through hydrogen bonding.

A successful example is the co-assembly of perylene tetracarboxylic di-imide (PTCDI, Fig. 13a) and melamine (Fig. 13b) on Ag/Si(1 1 1)-$\sqrt{3} \times \sqrt{3}$R30° under UHV conditions, shown in Fig. 13, as reported by Theobald et al. [106]. All HBs involved in the 2D MPNs formed were established between the PTCDI and melamine molecules. Highly ordered 2D hexagonal MPNs were prepared by sequential depositions of PTCDI and melamine molecules onto the substrate. The substrate temperature was kept at about 100 °C to supply sufficient energy to mobilize the PTCDI molecules at the surface to form HBs with melamine molecules during melamine deposition (Fig. 13c). The 2D hexagonal MPNs prepared as such could at most cover 50% of the substrate (Fig. 13d–g), and the hexagonal pores were big enough to accommodate a number of guest molecules. The guest molecules could be the PTCDI molecule itself when PTCDI was deposited during or after the formation of the 2D MPNs, or a cluster of 2–7 fullerenes after the deposition of fullerene that typically formed heptamers in a compact way in the 2D MPNs. A second fullerene layer was formed as the fullerene cov-

erage reached above one monolayer, showing the same hexagonal pattern which sat exactly on top of the PTCDI–melamine network. This represents a family of typical binary donor–acceptor systems [80–82] established via conventional hydrogen bonding.

The same bi-molecular system was also studied in detail on Au(1 1 1) [107], resulting, after annealing at 60–80 °C, in similar hexagonal 2D MPNs as well as some other unusual patterns. The original hexagonal MPNs gradually converted into parallelogram ones after further thermal treatment at about 90 °C [108]. As a step further, Br- and propylthio-substituted PTCDI molecules were employed to study the effects of side groups on network formation and accommodation on Ag/Si(1 1 1)-$\sqrt{3} \times \sqrt{3}$R30° [109].

In addition to the PTCDI–melamine binary system, some other analogues were also introduced into such bi-molecular studies [54,110–112]. It is noted that hydrogen bonding between fluorine and hydrogen atoms could also be employed to construct 2D MPNs [113] that used di-indenoperylene (DIP) and fluorinated copper-phthalocyanine (F_{16}CuPc) as the building blocks.

2.2.2.2. Metal–ligand coordination. Bi-molecular systems formed through pure metal–ligand coordination are still in their early stage. One possible reason is that the coordination strengths among different ligands are different, leading to different domains of coordinated 2D MPNs. Therefore, 2D MPNs constructed by the coordination between one metal core and two different ligands seem very unusual. Such an unusual case is reported by Lin et al. [114] who used bis(4-pyridyl)-1,4-benzene (**1**) and (2,2′-bipyridine)-5,5′-dicarboxylic acid (**2**) as ligands to coordinate with Cu adatoms on Cu(1 0 0) surface under UHV conditions, as schematically shown in Fig. 14a. One of the ligands coordinated along and the other, perpendicular to the molecular axis, resulting in dumbbell-shaped units, Cu_2(**1**)(**2**)$_2$. Two stacking styles of the dumbbell-shaped units (Fig. 14b and c) were observed on the atomically flat, defect-free and atomically stepped surfaces, respectively. The dumbbell-shaped units were connected by hydrogen bonding at different positions of the ligands, introducing additional hierarchical interactions to stabilize the whole 2D MPNs. Interestingly, ligand **2** in excess could serve as a guest molecule that drastically disturbed the 2D MPNs formed.

2.2.2.3. Chemical bonding. Covalent bonds also work for bi-molecular systems. In fact, Ref. [97] has already indicated a simple bi-molecular chemical reaction between BDBA and HHTP. Another piece of work accomplished by Weigelt et al. [115] realizes the condensation reaction between aldehyde and aliphatic amine on a Au(1 1 1) surface under UHV conditions, as shown in Fig. 15. Initially, dialdehyde was deposited onto the inert substrate at submonolayer coverage, forming well ordered patterns. Then, the sample was exposed to octylamine vapor at room temperature. The *in situ* surface reaction was confirmed by the resemblance of the surface structures after *in situ* and *ex situ* surface reactions, according to spectroscopic measurements by near-edge X-ray absorption fine structure (NEXAFS), and gradual ordering of the porous network during the surface reaction. Further annealing the sample at 400–450 K led to larger domains of such ordered structures. Similarly, this reaction was carried out at room temperature, indicating a low energy barrier for the surface reaction. This would give us much flexibility to tune and prepare more stable and complicated 2D MPNs.

In summary, while the knowledge for the preparations and controls of the uni-molecular MPNs has been essentially established, exploration of bi-molecular MPNs is at its early stage. Many uncertainties relating to the 2D binary MPNs are yet to be clarified. Comprehensive tuning and control of the complex binary MPNs are still a long way to go.

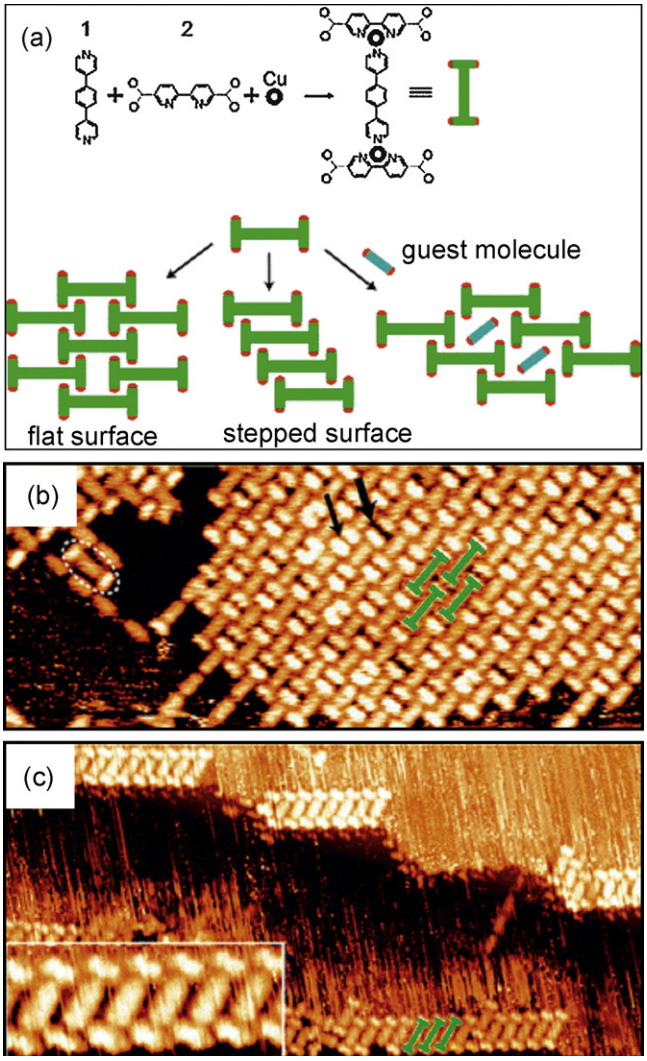

Fig. 14. (a) Schematic diagram of the coordinated dumbbell-like building block in green (consisting of one molecule **1**, two molecules **2** and two Cu atoms), together with three possible assembled structures constructed by the building block or with a guest molecule in light blue; (b) the assembling structure on the flat terrace of Cu(1 0 0) (33 nm × 14 nm, the building block is marked by the dash circle, and arrows indicating defects of missed molecule **1**); (c) the assembling structure at steps (44 nm × 22 nm). Reprinted with permission from [114]. ©Royal Chemical Society (2007).

3. External factors

Here, the external factors affecting the 2D MPNs are mainly defined as the substrate, solvent and external field effects. The solvent effect merely applies to the assembling processes at liquid/solid interfaces.

Substrates can strongly influence the structure of a 2D MPN by changing the molecule–substrate interaction which subsequently disturbs the overall balance of various interactions involved in the whole system. To minimize the substrate effect, atomically flat and chemically inert substrates are frequently used. HOPG and Au(1 1 1) are two of the most frequently used substrates for STM investigation either in liquid environments or under UHV conditions, owing to their chemical inertness and ease of preparation. For surface coordination and chemical bonding, some chemically active substrates such as Cu, Pt and Ru single crystals may be utilized. For example, Cu adatoms on Cu(1 0 0) serve as the metal cores to form coordination complexes [85], and Pt(1 1 1) surface can successfully catalyze the dehydrogenation reaction to directly synthesize fullerene in

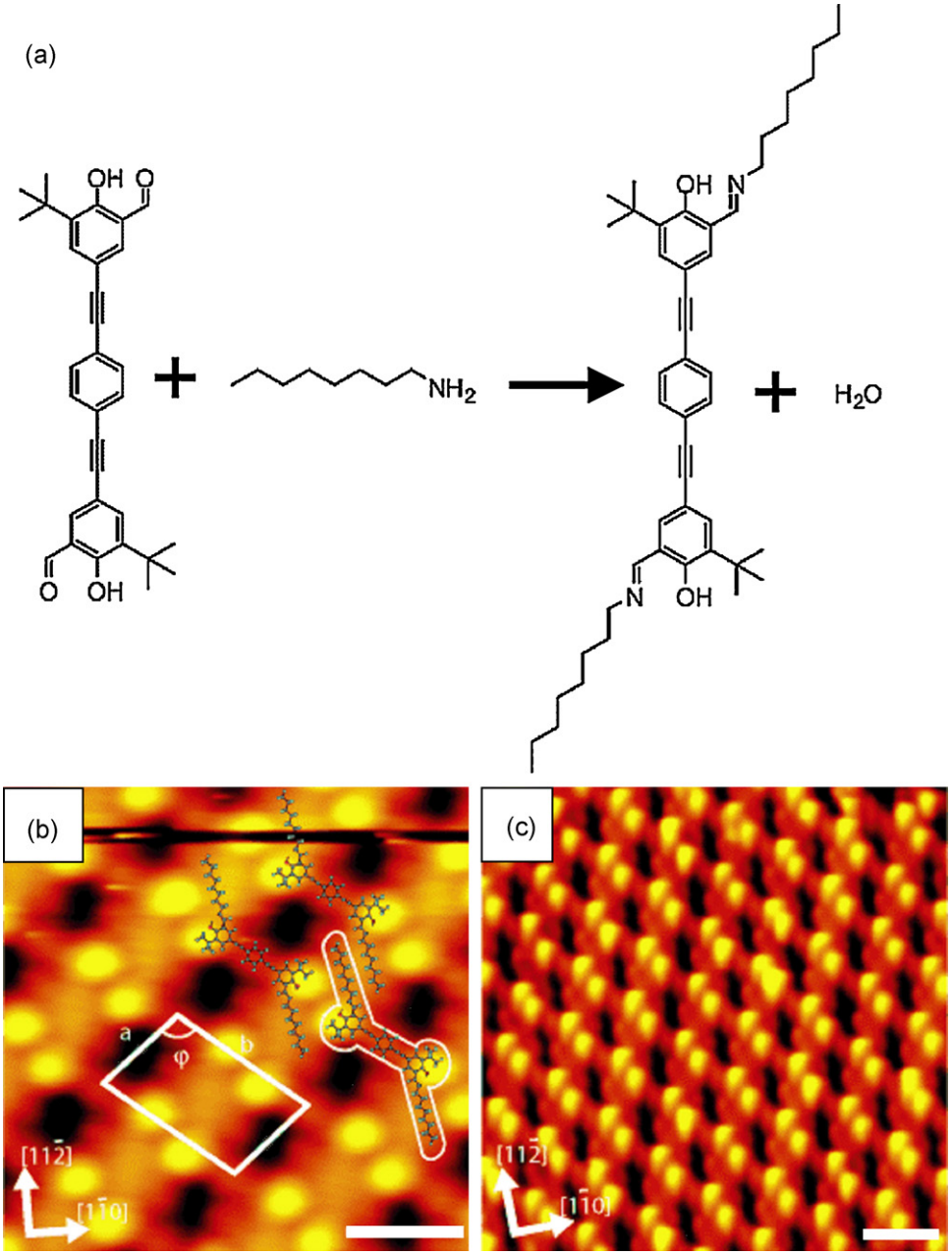

Fig. 15. (a) Chemical reaction formula of dialdehyde and octylamine; (b) high-resolution STM topograph of the assembled products (scale bar, 2 nm) with the modeled product molecules superimposed and the unit cell marked by the white frame and (c) large-area STM image (scale bar, 4 nm). Adapted from [115]. ©John-Wiley (2007).

two dimensions [116]. However, most molecular self-assemblies are constructed through non-covalent interactions which are energetically less favorable, chemically reactive substrates are usually discarded. Except for the non-conducting mica, no oxide single crystals have been used as substrates to prepare molecular self-assemblies, not to mention 2D MPNs.

In contrast to the universal availability of the substrate effect, the solvent effect only exists in liquid environments. The reason is obvious because the solvent would contribute through the molecule–solvent interaction to the overall balance of interactions. Solvents can influence the final assembling structures at the liquid/solid interfaces via properties such as polarity, solvation and viscosity [117]. These solvent properties in turn can be used to tune and control the assembling structures at the liquid/solid interface.

The external field effect can refer to the external electric and magnetic fields. An external electric field may force the assembly of molecules, especially polar ones, to stay at the surfaces. It is one of the main driving forces for ECSTM applied to study molecular assemblies. Wang and Wan [118] has already reviewed the applications of ECSTM in studies of surface assemblies. There are scarce reports on the application of an external magnetic field to tune and control molecular assemblies, although in principle there is no reason not to do this for self-assemblies of magnetic molecules.

To limit our discussions, we hereafter only discuss the substrate and solvent effects.

3.1. Substrate effect

The substrate effect in 2D MPNs lacks systematic investigation. Theoretically, the molecule–substrate interaction and the substrate lattice symmetry can directly influence 2D MPN structures. Chemically speaking, if a substrate strongly interacts with the assembled

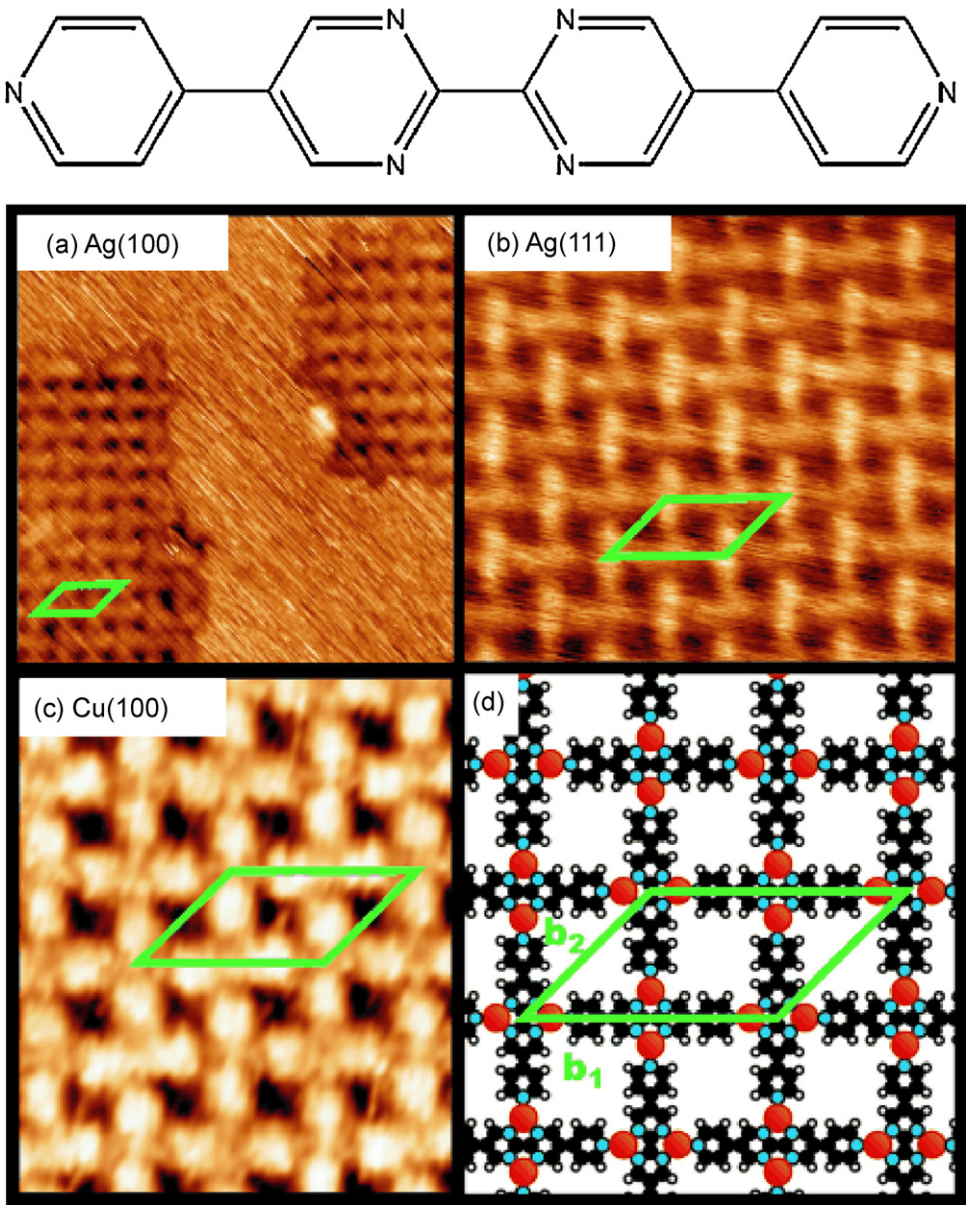

Fig. 16. STM images of the Cu–PBP coordinated structures on (a) Ag(1 0 0), 15.0 nm × 16.0 nm; (b) Ag(1 1 1), 10.8 nm × 10.1 nm and (c) Cu(1 0 0), 5.2 nm × 6.3 nm; (d) schematic molecular model of the coordinated structure. Green frames indicate the unit cell. On top is the molecular structure of PBP. Adapted from [119]. ©John-Wiley (2008).

molecule to such an extent that a chemical bond establishes, then the mobility of the molecule is greatly limited and hence, molecular assembly can hardly form at the surface.

Recently, Tait et al. [119] have tried to tackle this issue. They used three substrates including Cu(1 0 0), Ag(1 0 0) and Ag(1 1 1) that possess different lattice constants and symmetries, as shown in Fig. 16. A coordinated network was chosen as the model system to explore the substrate effect in which 5,5′-bis(4-pyridyl)(2,2′-bipyrimidine) (PBP) was employed as the ligand and Cu, as the metal core. The ligand could self-assemble into close-packed row structures on both Ag(1 0 0) and Ag(1 1 1). Deposition of Cu atoms onto the surfaces with submonolayer PBP and subsequent annealing at 400 K successfully resulted in well ordered 2D MPNs. However, this coordination system formed nearly identical 2D square MPNs on all three substrates, indicating that the molecule–substrate interactions on three substrates were not strong enough to drive the structural changes of the networks. Such a strong coordination was attributed to one additional Cu–N coordination number, in sharp contrast with previous result [104].

Further examples are the TMA assemblies on HOPG and Au(1 1 1) [29,32,120]. On HOPG, only the chicken-wire and flower porous structures can be formed, but a series of other higher order assembling structures from $H_{TMA\text{-}3}$ to $H_{TMA\text{-}8}$ and $H_{TMA\text{-}\infty}$ can be feasibly prepared on Au(1 1 1). This comparison implies that the TMA–Au interaction is stronger than TMA–HOPG because the molecular density stepwise increases with the structural evolution from the chicken-wire structure to higher order ones. Only a stronger TMA–Au interaction could force TMA molecules to stick to the surface under the same experimental conditions.

The above descriptions demonstrate that the substrate has to be carefully chosen in order to make the best compromise among all interactions. This can be utilized to tune and control 2D MPNs at the surface. It can be safely deduced that 2D MPNs constructed by chemical bonding between the assembled molecules are seldom influenced by substrates (if the substrate does not serve as a catalyst), and those prepared by weak non-covalent interactions can be efficiently affected by substrates.

3.2. Solvent effect

In liquid environments, solvents sometimes play a key role in tuning and controlling the 2D MPNs. A convincing example is given by Lackinger et al. [120]. A series of alkanoic acids from butyric to nonanoic acid were used as the solvents during the TMA assembly on HOPG. Interestingly, the flower structure was only formed in the solvent acids with shorter alkyl chains, including butyric, pentanoic and hexanoic acids. In contrast, the chicken-wire structure only existed in octanoic and nonanoic acids. However, both structures were identified in heptanoic acid. According to the authors' speculations, the shorter-chained acids favor the formation of TMA trimers which exist in the flower structure.

In our previous study [117], we have shown that two self-assembled structures, the V- and Z-shaped molecular configurations, of 3,8-bis-hexadecyloxy-benzo [c]cinnoline (BC16) appeared on HOPG. The relative ratio of the two molecular configurations varied with the solvents used. Only the Z-shaped molecular configuration (with a higher dipolar moment) existed in non-polar solvents such as 1-phenyloctane, carbon tetrachloride and toluene while it co-existed with the V-shaped molecular configuration (with a lower dipolar moment) in polar solvents like 1-octanol, chloroform and 1,2-dichloroethane. This implies that for an assembling molecule with different configurations of different polarities, the polar configuration normally survives in non-polar solvents and assembles at the surface because non-polar configurations are dragged into solution by non-polar solvents, and *vice versa*. We may name this as a similarity rule for surface assemblies in liquid environments.

In addition to the systematic studies mentioned above, on the solvent effect, several scattered reports also showed the solvent effects on different self-assembled architectures [37,121–123].

4. Applications of molecular porous networks

It has long been anticipated that highly ordered 2D MPNs are promising for applications in nanofabrication and mediations of surface reactions. These 2D MPNs are essentially employed as host systems (i.e., secondary templates) such as calix [8]arene derivatives, TMA, porphyrin derivatives, phthalocyanine derivatives, cyclothiophenes, and many other molecular building blocks described above. Their nanopores can obviously hold alien ensembles. For instance, a cavity surrounded by six porphyrins can be occupied by a single porphyrin molecule that sits at six equivalent locations in the framework of a sixfold symmetric site [124]. Another example is that in the TMA 2D MPNs, a TMA molecule itself can be trapped in the cavity available in both chicken-wire and flower structures, as studied by Griessl et al. [27].

Examples of some alien ensembles hosted by 2D MPNs include fullerenes-C_{60} [91,125–129], C_{84}, C_{70}, C_{120}, C_{130} and C_{180} [128]. Some guest molecules can be located either in nanopores or on top of the 2D MPNs through donor–acceptor interaction between the bithiophene-based MPN and C_{60} [71].

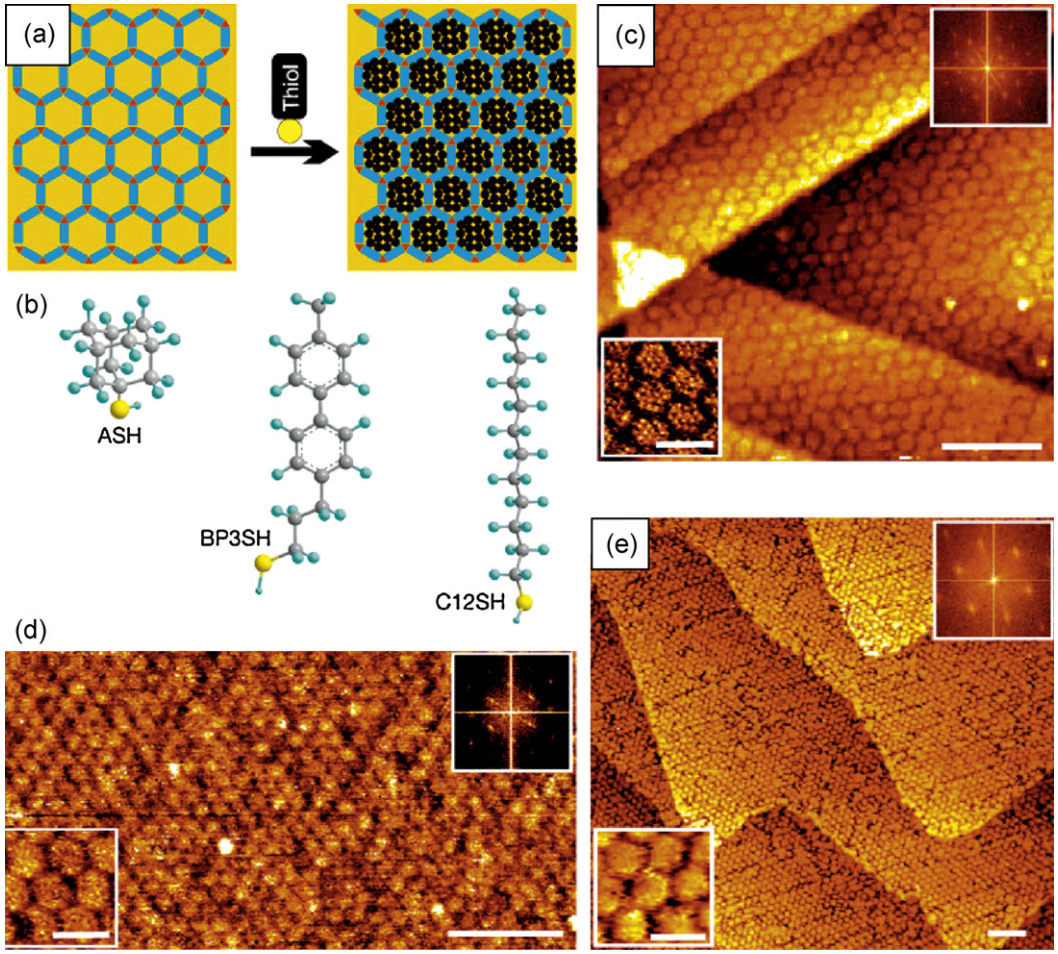

Fig. 17. Thiols engrafted in the nanopores of the PTCDI–melamine MPNs formed on Au(1 1 1)/mica substrate. (a) Schematic diagram of the MPNs filled with thiols; (b) three thiol molecules, ASH, C12SH and BP3SH, used to fill the MPN pores; (c)–(e) STM images of the MPNs filled with ASH, C12SH and BP3SH, respectively. The insets at the lower left and upper right corners of the STM images are high-resolution images and Fourier transforms, respectively. Scale bars for large pictures: 20 nm, and scale bars for insets: 5 nm. Reprinted with permission from [130]. ©Nature Publishing Group (2008).

The assembling molecules in 2D MPNs may act as guest molecule spacers and participants in a chemical reaction (see context hereafter). Simply speaking, the pore wall can prevent guest ensembles from meeting outside species like coronene in TMA MPN [32], C_{60} in calix [8]arene MPN [67] and cyclo [12]thiophene MPN [72].

At certain coverages of the guest molecules, it is possible to build up more complex structures atop the mixed monolayer. For example, Theobald et al. [106] fabricated a MPN (a bi-molecular one by PTCDI and melamine) with its pores filled by C_{60}-heptamers. Further supply of C_{60} molecules led to the adsorption of excess C_{60} molecules on MPN walls, generating a second layer of fullerenes that duplicates the underlying porous network structure.

2D MPNs can precisely control the locations of the guest molecules, which may have great potential application in the future. Madueno et al. [130] achieved a multi-layered network based on the PTCDI–melamine honeycomb layer. Initially, they immersed a Au(1 1 1)/mica substrate in the saturated solution of PTCDI/melamine. Afterwards, they lifted up and dried the sample to obtain a bi-molecular MPN. Then the sample was again immersed in dilute thiol solutions to obtain modified MPNs since thiols were adsorbed on exposed Au inside the 2D MPN pores. Afterwards, Cu(II) ions were electrically deposited onto the surface. The Cu atoms inserted between the thiols and substrates, resulting in confined metal-deposition structures on Au(1 1 1) (Fig. 17). By using the solution approach, surface modifications exhibit flexibilities compared with those carried out under UHV conditions. It is likely that a combination of 2D MPNs and self-assembled monolayers (SAMs) might be helpful in building other supramolecular structures with a nanometric precision.

There exist also some epitaxially grown hierarchical assemblies. For example, fullerenes preferentially adsorb at the interspaces in a self-assembled coronene layer on Au(1 1 1). Excess fullerenes can further assemble into a second layer atop the underlying mixed layer. Further, ZnOEP and zinc phthalocyanine (ZnPc) coadsorbed on Au form mixed monolayers with C_{60} selectively localized at centers of every two pairs of blocks on a so-called "chessboard" pattern of ZnOEP/ZnPc SAM [131]. Apart from these, a bowl-like molecule corannulene with suitable size to accommodate C_{60} forms a 2D MPN on Cu(1 1 0) in vacuum, yielding a "buckybowl-buckyball" host–guest system [132]. It is quite possible to synthesize some special and applicable structures for nanodevices in those systems where guest molecules can engage in forming 2D MPNs, i.e., the guest-induced nanoporous structures [39,133] and a SAM of a C_{60}-derivative (phenyl-C_{61}-butyric acid methyl ester) on Au(1 1 1) [134].

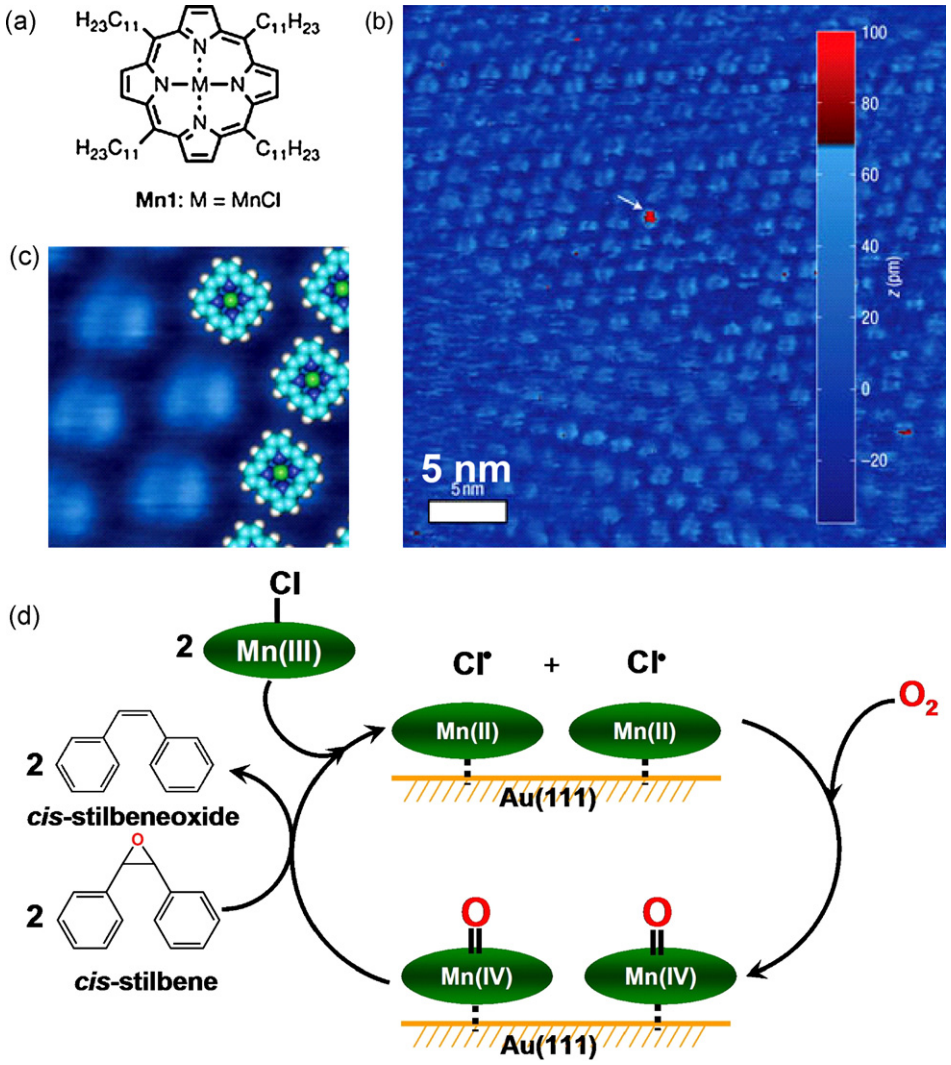

Fig. 18. (a) Molecular structure of **Mn1**; (b) STM image of a monolayer of **Mn1** self-assembled at the liquid–solid interface of Au(1 1 1) and argon-saturated *n*-tetradecane (color bar at the right side indicating the apparent height in STM, and the white arrow showing a molecule with much higher apparent height); (c) enlarged STM image of the **Mn1** assembly with the modeled molecules superimposed. (d) Proposed catalytic cycle of the *cis*-stilbene epoxidation at the interface of Mn(III)-porphyrin chloride SAM and the solution of *n*-tetradecane on Au(1 1 1). Adapted from [139]. ©Nature Publishing Group (2007).

In addition, guest molecules can also tune the 2D MPNs by enlarging the pore size [135], deforming the pore shape [43] and modifying the assembly patterns [25], due to the interplays among various interactions.

The thermodynamics and kinetics in host–guest systems are being extensively studied. Motions of molecules adsorbed on porous networks are commonly known as rotation, diffusion and assembling. In the pores of dehydro-DPDI monolayer, ZnOEP exhibits thermally activated rotation libration [84]. Nanographene molecules in a DBA derivative-SAM pore can rotate with respect to the central axis of the pore, meanwhile the number of aggregated members within a single pore changed [136]. Molecules trapped in pores aggregating into clusters have been reported by Theobald et al. [137] and Furukawa et al. [39]. Guest molecules hopping between pores are observed in the coronene-incorporated 1,3,5-tris [(*E*)-2-(3,5-didecyloxyphenyl)-ethenyl]-benzene (TSB35) MPN [138] and C_{60}-incorporated TMA MPN. The latter is termed as "playing nanosoccer" by Griessl et al. [31]. Since the adsorption of molecules at liquid–solid interface is a dynamic process, the cavities in a 2D MPN on the substrate can be reoccupied by molecules from solution. This has been reported by Griessl et al. [32].

A chemical process taking place in the 2D MPNs may be influenced by the assembling molecules. First, the location and conformation of a reactant depend on its interactions with the MPN and substrate. Therefore, the chemical nature of the MPN may play an important role in mobilizing an adsorbate, which in turn influences a reaction process. Second, the pore structure can spatially confine the guest molecules, thus the reactant reactivity may be different from that in solution or bulk. Hulsken et al. [139] used the self-assembly of Mn(III)-porphyrin chloride (**Mn1**) to catalyze the *cis*-stilbene epoxidation at the interface of Au(1 1 1) and argon-saturated *n*-tetradecane solution, as shown in Fig. 18. Although it did not achieve a high performance, this reaction did show, to a certain extent, a *cis*-isomer selectivity. The UV–vis spectroscopy captured a blue-shift of the Soret band, showing the interaction between the substrate and the metal center in the self-assembly. After flushing the bell jar initially full of argon atmosphere with O_2, the **Mn1** molecules on the substrate were gradually oxidized. The reaction process was monitored *in situ* by STM and gas chromatography. The mechanism involves the splitting of O_2 (through redox reactions between the O_2 and Mn(II) species) into two oxygen atoms which subsequently anchored to a pair of adjacent Mn(IV) ions. These then oxidized the *cis*-stilbene ethylene groups, leaving reduced metal–porphyrin residues on the substrate, as indicated by real-time STM measurements. This experiment shed light on exploiting 2D MPNs for chemical reactions.

2D MPNs can also have some other interesting applications. Kim et al. [140] prepared a pseudo-2D MPN with cucurbituril molecules on gold. Each pore was threaded by a chain molecule anchored to the gold surface with a 1,2-dithiolane group. The assembly of the pseudorotaxanes could undergo threading and dethreading processes. When the cucurbituril molecules were dethreaded, it allowed $[Fe(CN)_6]^{3-}$ to access the substrate, suggesting that the cavitands (cucrubiturils) acted as "gates" preventing the ions from entering the inner space between the chains. The working mechanism could be controlled by using solutions of different pH value, facilitating the cavitands to assemble into a supramolecular array or to disappear from the array.

Versatile molecules such as porphyrin derivatives can be used for rational design of functional supramolecular assemblies. A marvelous example by Lee et al. [141] demonstrated a type of porphyrin-box assembled through a "self-sorting strategy", which possessed catalytically active sites triggering size-selective and enantioselective oxidation of *cis*-stilbenes and methyl *p*-tolyl sulfide, respectively. This may be applied in supramolecular engineering. Moreover, within a pore in the 2D MPNs, a single event of molecular transformation and other motions involved in the reactions could be identified.

In general, the size, shape and chemical nature of the pores and the inter-pore distance in 2D MPNs can be utilized to explore various host–guest systems, to construct hierarchical assembling structures and to chemically control adsorption and reaction of molecules.

5. Summaries and perspectives

Because of their promising applications and possible tunability and controllability, 2D MPNs have become representative systems in surface assemblies. Molecular self-assembling has long been thought of in nanoscience and nanotechnology as an efficient approach, the so-called "bottom-up" approach, to preparing nanostructures. However, this approach will not work without realistic control. After several years of striving efforts, people have reached the consensus that 2D MPNs might be the model system that satisfies the requirements mentioned above, and hence, could serve as secondary templates to host alien ensembles, as spatial confiners to control chemical reactions, as molecular sensors for chemical and biological detections, etc.

To construct the 2D MPNs, various surface assembling approaches have been developed that work either under UHV conditions or in liquid environments. The tuning and control of the 2D MPN structures involve tweaking the balance of various interactions among the assembling molecules, substrate and/or solvents, depending on the working surroundings, namely, in vacuum or solution. To realize control of the 2D MPNs, various building blocks have been selected, where linear or non-linear and planar or non-planar organic molecules have been employed. The basic selection rules lie in two aspects: the structural geometries of the assembling molecules that can determine the dimensions of the 2D MPNs, and the functional groups in the assembling molecules that dictate the balanced interactions involved in the 2D MPNs. To achieve the 2D MPNs, the assembling molecules or building blocks must not be strongly adsorbed, i.e., chemically bonded, at the surfaces because this would restrict the mobility of the molecules. To realize periodic arrangements, the molecules have to be mobile at the surfaces so that they can find the suitable surface locations in order to minimize the overall energy of the system.

To tune and control the 2D MPN structures, both internal and external factors can be used. The internal factors are the building blocks (or assembling molecules) and inter-molecule interactions, while the external ones are substrates, solvents and external electric and magnetic fields. In addition to the external factors, the focus is usually on tweaking the weak interactions of the assembling molecules. In this sense, researchers have experimentally and theoretically checked the strengths of the inter-molecular interactions comprising mainly vdW forces, dipole–dipole coupling, hydrogen bonding and metal–ligand coordination. Without directionality, the former two interactions are not extensively utilized in constructing 2D MPNs. Therefore, a majority of work rely on the latter two interactions, hydrogen bonding and metal–ligand coordination, to prepare 2D MPNs. People have scrutinized various hydrogen-bonded structures and found that molecules with functional groups like –COOH, –OH and $-NH_x$ ($x \geq 1$) are efficient candidates. In terms of the metal–ligand coordination, ligands with functional groups such as –COOH and –N= are proven to be good ones, while the metal cores so far tested are only Fe, Co, Mn and Cu.

Although various 2D MPNs have been reported in the literature, few are really predictable. The only exception is the TMA-based 2D MPNs whose structures can be theoretically predicted, albeit qualitatively, through an energy analysis.

In terms of their stability, weakly bonded 2D MPNs are obviously fragile to external perturbations like vigorous STM tip scanning or thermal treatments. To enhance the stability, the molecules are better held together by chemical bonds. Therefore, chemically bonded 2D MPNs have generated some interest in the past couple of years.

As stated before, the main driving force to develop various 2D MPNs is their potential and promising applications in various fields. Until now, 2D MPNs are mainly used as secondary templates to host alien ensembles to prepare periodically arranged nanoarrays. The spherical fullerenes and their derivatives, planar coronene and other molecules like TMA, phthalocyanines and porphyrins, and some metal ions are the commonly hosted ensembles. Another appealing application of the 2D MPNs is that the microcavities inside serve as a confined cavity reactor for chemical reactions, i.e., 2D Mn(III)-porphyrin chloride MPN to catalyze the *cis*-stilbene epoxidation on Au(1 1 1).

With the exciting achievements, described above, for 2D MPNs, one has to admit that to fully realize controllability, predictability, stability and applicability, we still have a long way to go. There are many aspects that are not even touched upon so far. No unimolecular MPNs other than the TMA-based one can be really tuned and controlled with a single simple parameter like surface coverage. In order to tune and control the 2D MPNs, the assembling molecule structure must be modified and rebuilt by changing its size or attaching additional functional groups. For bi-molecular systems, it is even harder to do so without destroying the network pattern.

One difficulty in the preparation of 2D MPNs by metal–ligand coordination is to enrich the types of metal cores. Metal atoms and ions with planar coordination capabilities could be feasibly implanted to prepare 2D MPNs, but most metal atoms and ions are coordinated in non-planar ways. Rare earth metal atoms and ions are expected to be useful in magnetism and spintronics. How to prepare 2D MPNs containing rare earth metals remains a tough and unresolved issue.

Although the assembling molecule can adopt chiral conformations in 2D MPNs, the networks are generally racemic. Some studies have shown that chiral MPNs could be fabricated. However, chiral MPNs with applications such as chiral synthesis, enzyme-mimic catalysis, etc. are rarely obtained. To build 2D MPNs from achiral and prochiral molecules, more experiments are needed in the future.

To use the surface assembling process as an efficient approach in the nanofield, large area 2D MPNs have to be prepared and be capable of crossing surface steps without changing their structures and periodicities. Until now, people can only achieve 2D MPNs on atomically flat surfaces which are rare in nature. To construct 2D MPNs on stepped and even roughened surfaces may be a new direction in the future. Conceptually, this is doable, the question is how?

For applications, simple hosting of some ensembles is a mere demonstration of the concept in host–guest systems. More useful ensembles with unique properties have to be used. At least, the 2D MPNs can be used to study coupling effects among the trapped ensembles. It is anticipated that 2D MPNs might be extensively employed to study spintronics and molspintronics that are very hopeful for information storage.

Needless to say, constructing 2D MPNs with pores that show confining and quantum effects to tune and control chemical reactions inside is very interesting to chemists. Whether it is achievable largely depends on how far scientists can go in the near future.

In summary, studies on 2D MPNs are of fundamental importance for us to understand the governing principles for self-assemblies. 2D MPNs are unique for exploring the controllability, predictability, stability and applicability of the ordered structures constructed by surface assembly.

Acknowledgements

This work is jointly supported by NSFC (20573001, 50821061, 20773001, 20827002) and MOST (2006CB806102, 2007CB936202, 2009CB929403), China.

References

[1] R. Garcia, R.V. Martinez, J. Martinez, Chem. Soc. Rev. 35 (2006) 29.
[2] M. Haga, K. Kobayashi, K. Terada, Coord. Chem. Rev. 251 (2007) 2688.
[3] D. Fichou, J. Mater. Chem. 10 (2000) 571.
[4] N. Koch, ChemPhysChem 8 (2007) 1438.
[5] A.C. Grimsdale, K. Müllen, Angew. Chem. Int. Ed. 44 (2005) 5592.
[6] M. Dincă, J.R. Long, Angew. Chem. Int. Ed. 47 (2008) 6766.
[7] J.V. Barth, Annu. Rev. Phys. Chem. 58 (2007) 375.
[8] K. Ariga, J.P. Hill, M.V. Lee, A. Vinu, R. Charvet, S. Acharya, Sci. Technol. Adv. Mater. 9 (2008) 014109.
[9] S. De Feyter, F.C. De Schryver, J. Phys. Chem. B 109 (2005) 4290.
[10] F. Rosei, M. Schunack, Y. Naitoh, P. Jiang, A. Gourdon, E. Laegsgaard, I. Stensgaard, C. Joachim, F. Besenbacher, Prog. Surf. Sci. 71 (2003) 95.
[11] J.V. Barth, G. Costantini, K. Kern, Nature 437 (2005) 671.
[12] F. Cicoira, C. Santato, F. Rosei, Top. Curr. Chem. 285 (2008) 203.
[13] N. Miyashita, D.G. Kurth, J. Mater. Chem. 18 (2008) 2636.
[14] L.J. Wan, Acc. Chem. Res. 39 (2006) 334.
[15] Y.F. Wang, Y.Y. Ye, K. Wu, Surf. Sci. 600 (2006) 729.
[16] L. Grill, J. Phys.: Condens. Matter. 20 (2008) 053001.
[17] R.K. Smith, P.A. Lweis, P.S. Weiss, Prog. Surf. Sci. 75 (2004) 1.
[18] J.I. Paredes, A. Martínez-Alonso, J.M.D. Tascón, Micropor. Mesopor. Mater. 65 (2003) 93.
[19] D. Bonifazi, A. Kiebele, M. Stöhr, F.Y. Cheng, T. Jung, F. Diederich, H. Spillmann, Adv. Funct. Mater. 17 (2007) 1051.
[20] S. Yoshimoto, K. Itaya, J. Porphyr. Phthalocya. 11 (2007) 313.
[21] T. Yokoyama, T. Kamidado, S. Yokoyama, S. Mashiko, J. Chem. Phys. 121 (2004) 11993.
[22] T. Yokoyama, S. Yokoyama, T. Kamikado, Y. Okuno, S. Mashiko, Nature 413 (2001) 619.
[23] T. Terui, S. Yokoyama, H. Suzuki, S. Mashiko, M. Sakurai, T. Moriwaki, Thin Solid Films 499 (2006) 157.
[24] F. Nishiyama, T. Yokoyama, T. Kamikado, S. Yokoyama, S. Mashiko, Appl. Phys. Lett. 88 (2006) 253113.
[25] F. Nishiyama, T. Yokoyama, T. Kamikado, S. Yokoyama, S. Mashiko, K. Sakaguchi, K. Kikuchi, Adv. Mater. 19 (2007) 117.
[26] A. Dmitriev, N. Lin, J. Weckesser, J.V. Barth, K. Kern, J. Phys. Chem. B 106 (2002) 6907.
[27] S. Griessl, M. Lackinger, M. Edelwirth, M. Hietschold, W.M. Heckl, Single Mol. 3 (2002) 25.
[28] G. Sheerin, A.A. Cafolla, Surf. Sci. 577 (2005) 211.
[29] Y.C. Ye, W. Sun, Y.F. Wang, X. Shao, X.G. Xu, F. Cheng, J.L. Li, K. Wu, J. Phys. Chem. C 111 (2007) 10138.
[30] D. Payer, A. Comisso, A. Dmitriev, T. Strunskus, N. Lin, C. Wöll, A.D. Vita, J.V. Barth, K. Kern, Chem. Eur. J. 13 (2007) 3900.
[31] S.J.H. Griessl, M. Lackinger, F. Jamitzky, T. Markert, M. Hietschold, W.M. Heckl, J. Phys. Chem. B 108 (2004) 11556.
[32] S.J.H. Griessl, M. Lackinger, F. Jamitzky, T. Markert, M. Hietschold, W.M. Heckl, Langmuir 20 (2004) 9403.
[33] H.J. Yan, J. Lu, L.J. Wan, C.L. Bai, J. Phys. Chem. B 108 (2004) 11251.
[34] K. Kannappan, T.L. Werblowsky, K.T. Rim, B.J. Berne, G.W. Flynn, J. Phys. Chem. B 111 (2007) 6634.
[35] J. Lu, Q.D. Zeng, C. Wang, Q.Y. Zheng, L.J. Wan, C.L. Bai, J. Mater. Chem. 12 (2002) 2856.
[36] M. Ruben, D. Payer, A. Landa, A. Comisso, C. Gattinoni, N. Lin, J.P. Collin, J.P. Sauvage, A.D. Vita, K. Kern, J. Am. Chem. Soc. 128 (2006) 15644.
[37] L. Kampschulte, M. Lackinger, A.K. Maier, R.S.K. Kishore, S. Griessl, M. Schmittel, W.M. Heckl, J. Phys. Chem. B 110 (2006) 10829.
[38] H. Zhou, H. Dang, J.H. Yi, A. Nanci, A. Rochefort, J.D. Wuest, J. Am. Chem. Soc. 129 (2007) 13774.
[39] S. Furukawa, K. Tahara, F.C. De Schryver, M.V.D. Auweraer, Y. Tobe, S. De Feyter, Angew. Chem. Int. Ed. 46 (2007) 2831.
[40] K. Tahara, S. Furukawa, H. Uji-i, T. Uchino, T. Ichikawa, J. Zhang, W. Mamdouh, M. Sonoda, F.C. De Schryver, S. De Feyter, Y. Tobe, J. Am. Chem. Soc. 128 (2006) 16613.
[41] S. Furukawa, H. Uji-i, K. Tahara, T. Ichikawa, M. Sonoda, F.C. De Schryver, Y. Tobe, S. De Feyter, J. Am. Chem. Soc. 128 (2006) 3502.
[42] S.B. Lei, K. Tahara, F.C. De Schryver, M.V.D. Auweraer, Y. Tobe, S. De Feyter, Angew. Chem. Int. Ed. 47 (2008) 2964.
[43] X.J. Ma, Y.L. Yang, K. Deng, Q.D. Zeng, K.Q. Zhao, C. Wang, C.L. Bai, J. Mater. Chem. 18 (2008) 2074.
[44] W. Xu, M.D. Dong, H. Gersen, E. Rauls, S. Vázquez-Campos, M. Crego-Calama, D.N. Reinhoudt, E. Lægsgaard, I. Stensgaard, T.R. Linderoth, F. Besenbacher, Small 4 (2008) 1620.
[45] N. Wintjes, J. Hornung, J. Lobo-Checa, T. Voigt, T. Samuely, C. Thilgen, M. Stöhr, F. Diederich, T.A. Jung, Chem. Eur. J. 14 (2008) 5794.

[46] Y.H. Wei, K. Kannappan, G.W. Flynn, M.B. Zimmt, J. Am. Chem. Soc. 126 (2004) 5318.
[47] S. De Feyter, A. Gesquière, M. Klapper, K. Müllen, F.C. De Schryver, Nano Lett. 3 (2003) 1485.
[48] X. Shao, X.C. Luo, X.Q. Hu, K. Wu, J. Phys. Chem. B 110 (2006) 15393.
[49] L.P. Xu, J.R. Gong, L.J. Wan, T.G. Jiu, Y.L. Li, D.B. Zhu, K. Deng, J. Phys. Chem. B 110 (2006) 17043.
[50] S. Stepanow, N. Lin, J.V. Barth, K. Kern, J. Phys. Chem. B 110 (2006) 23472.
[51] U. Schlickum, R. Decker, F. Klappenberger, G. Zoppellaro, S. Klyatskaya, M. Ruben, I. Silanes, A. Arnau, K. Kern, H. Brune, J.V. Barth, Nano Lett. 7 (2007) 3813.
[52] D. Kühne, F. Klappenberger, R. Decker, U. Schlickum, H. Brune, S. Klyatskaya, M. Ruben, J.V. Barth, J. Am. Chem. Soc. 131 (2009) 3881.
[53] W.D. Xiao, X.L. Feng, P. Ruffieux, O. Gröning, K. Müllen, R. Fasel, J. Am. Chem. Soc. 130 (2008) 8910.
[54] P.A. Staniec, L.M.A. Perdigao, B.L. Rogers, N.R. Champness, P.H. Beton, J. Phys. Chem. C 111 (2007) 886.
[55] M. Schöck, R. Otero, S. Stojkovic, F. Hümmelink, A. Gourdon, E. Lægsgaard, I. Stensgaard, C. Joachim, F. Besenbacher, J. Phys. Chem. B 110 (2006) 12835.
[56] H. Spillmann, A. Dmitriev, N. Lin, P. Messina, J.V. Barth, K. Kern, J. Am. Chem. Soc. 125 (2003) 10725.
[57] P. Messina, A. Dmitriev, N. Lin, H. Spillmann, M. Abel, J.V. Barth, K. Kern, J. Am. Chem. Soc. 124 (2002) 14000.
[58] T. Classen, M. Lingenfelder, Y.L. Wang, R. Chopra, C. Virojanadara, U. Starke, G. Costantini, G. Fratesi, S. Fabris, S.D. Gironcoli, S. Baroni, S. Haq, R. Raval, K. Kern, J. Phys. Chem. A 111 (2007) 12589.
[59] W. Auwärter, A. Weber-Bargioni, A. Riemann, A. Schiffrin, O. Gröning, R. Fasel, J.V. Barth, J. Chem. Phys. 124 (2006) 194708.
[60] U. Schlickum, R. Decker, F. Klappenberger, G. Zoppellaro, S. Klyatskaya, W. Auwärter, S. Neppl, K. Kern, H. Brune, M. Ruben, J.V. Barth, J. Am. Chem. Soc. 130 (2008) 11778.
[61] N.A. Stephenson, A.T. Bell, J. Mol. Catal. A: Chem. 275 (2007) 54.
[62] S. Takagi, M. Eguchi, D.A. Tryk, H. Inoue, J. Photochem. Photobiol. C 7 (2006) 104.
[63] L. Valli, Adv. Colloid Interface Sci. 116 (2005) 13.
[64] P. Peumans, A. Yakimov, S.R. Forrest, J. Appl. Phys. 93 (2003) 3693.
[65] D. Kim, A. Osuka, J. Phys. Chem. A 107 (2003) 8791.
[66] D.M. Guldi, Chem. Soc. Rev. 31 (2002) 22.
[67] G.B. Pan, J.M. Liu, H.M. Zhang, L.J. Wan, Q.Y. Zheng, C.L. Bai, Angew. Chem. Int. Ed. 42 (2003) 2747.
[68] G.B. Pan, J.H. Bu, D. Wang, J.M. Liu, L.J. Wan, Q.Y. Zheng, C.L. Bai, J. Phys. Chem. B 107 (2003) 13111.
[69] G.B. Pan, L.J. Wan, Q.Y. Zheng, C.L. Bai, Chem. Phys. Lett. 367 (2003) 711.
[70] E. Mena-Osteritz, Adv. Mater. 14 (2002) 609.
[71] G.B. Pan, X.H. Cheng, S. Höger, W. Freyland, J. Am. Chem. Soc. 128 (2006) 4218.
[72] E. Mena-Osteritz, P. Bäuerle, Adv. Mater. 18 (2006) 447.
[73] J. Krömer, I. Rios-Carreras, G. Fuhrmann, C. Musch, M. Wunderlin, T. Debaerdemaeker, E. Mena-Osteritz, P. Bäuerle, Angew. Chem. Int. Ed. 39 (2000) 3481.
[74] J.A.R. Navarro, B. Lippert, Coord. Chem. Rev. 222 (2001) 219.
[75] O. Crespo-Biel, B.J. Ravoo, D.N. Reinhoudt, J. Huskens, J. Mater. Chem. 16 (2006) 3997.
[76] J. Lewiński, J. Zachara, I. Justyniak, M. Dranka, Coord. Chem. Rev. 249 (2005) 1185.
[77] C.F.J. Faul, M. Antonietti, Adv. Mater. 15 (2003) 673.
[78] L.J. Prins, D.N. Reinhoudt, P. Timmerman, Angew. Chem. Int. Ed. 40 (2001) 2382.
[79] A. Gourdon, Angew. Chem. Int. Ed. 47 (2008) 6950.
[80] D.A. Bell, E.V. Anslyn, Tetrahedron 51 (1995) 7161.
[81] G.R. Desiraju, Angew. Chem. Int. Ed. Engl. 34 (1995) 2311.
[82] H. Schneider, Angew. Chem. Int. Ed. Engl. 30 (1991) 1417.
[83] M. Stöhr, M. Wahl, C.H. Galka, T. Riehm, T.A. Jung, L.H. Gade, Angew. Chem. Int. Ed. 44 (2005) 7394.
[84] M. Stöhr, M. Wahl, H. Spillmann, L.H. Gade, T.A. Jung, Small 3 (2007) 1336.
[85] N. Lin, A. Dmitriev, J. Weckesser, J.V. Barth, K. Kern, Angew. Chem. Int. Ed. 41 (2002) 4779.
[86] A. Dmitriev, H. Spillmann, N. Lin, J.V. Barth, K. Kern, Angew. Chem. Int. Ed. 42 (2003) 2670.
[87] T. Classen, G. Fratesi, G. Costantini, S. Fabris, F.L. Stadler, C. Kim, S.D. Gironcoli, S. Baroni, K. Kern, Angew. Chem. Int. Ed. 44 (2005) 6142.
[88] S. Stepanow, N. Lin, D. Payer, U. Schlickum, F. Klappenberger, G. Zoppellaro, M. Ruben, H. Brune, J.V. Barth, K. Kern, Angew. Chem. Int. Ed. 46 (2007) 710.
[89] N. Lin, S. Stepanow, F. Vidal, J.V. Barth, K. Kern, Chem. Commun. (2005) 1681.
[90] M.A. Lingenfelder, H. Spillmann, A. Dmitriev, S. Stepanow, N. Lin, J.V. Barth, K. Kern, Chem. Eur. J. 10 (2004) 1913.
[91] S. Stepanow, M. Lingenfelder, A. Dmitriev, H. Spillmann, E. Delvigne, N. Lin, X. Deng, C. Cai, J.V. Barth, K. Kern, Nat. Mater. 3 (2004) 229.
[92] Y.F. Zhang, N. Zhu, T. Komeda, J. Phys. Chem. C 111 (2007) 16946.
[93] Y.F. Zhang, N. Zhu, T. Komeda, Surf. Sci. 602 (2008) 614.
[94] S.L. Tait, Y.L. Wang, G. Costantini, N. Lin, A. Baraldi, F. Esch, L. Petaccia, S. Lizzit, K. Kern, J. Am. Chem. Soc. 130 (2008) 2108.
[95] A.P. Seitsonen, M. Lingenfelder, H. Spillmann, A. Dmitriev, S. Stepanow, N. Lin, K. Kern, J.V. Barth, J. Am. Chem. Soc. 128 (2006) 5634.
[96] N. Lin, S. Stepanow, F. Vidal, K. Kern, M.S. Alam, S. Strömsdörfer, V. Dremov, P. Müller, A. Landa, M. Ruben, Dalton. Trans. (2006) 2794.
[97] N.A.A. Zwaneveld, R. Pawlak, M. Abel, D. Catalin, D. Gigmes, D. Bertin, L. Porte, J. Am. Chem. Soc. 130 (2008) 6678.
[98] L. Grill, M. Dyer, L. Lafferentz, M. Persson, M.V. Peters, S. Hecht, Nat. Nanotechnol. 2 (2007) 687.
[99] M. Matena, T. Riehm, M. Stöhr, T.A. Jung, L.H. Gade, Angew. Chem. Int. Ed. 47 (2008) 2414.
[100] M.I. Veld, P. Iavicoli, S. Haq, D.B. Amabilino, R. Raval, Chem. Commun. (2008) 1536.
[101] S. Weigelt, C. Bombis, C. Busse, M.M. Knudsen, K.V. Gothelf, E. Lægsgaard, F. Besenbacher, T.R. Linderoth, ACS Nano 2 (2008) 651.
[102] G.A. Somorjai, Introduction to Surface Chemistry and Catalysis, Wiley-Interscience, 1994.
[103] A. Langner, S.L. Tait, N. Lin, R. Chandrasekar, M. Ruben, K. Kern, Angew. Chem. Int. Ed. 47 (2008) 8835.
[104] S.L. Tait, A. Langner, N. Lin, S. Stepanow, C. Rajadurai, M. Ruben, K. Kern, J. Phys. Chem. C 111 (2007) 10982.
[105] A. Langner, S.L. Tait, N. Lin, C. Rajadurai, M. Ruben, K. Kern, PNAS 104 (2007) 17927.
[106] J.A. Theobald, N.S. Oxtoby, M.A. Phillips, N.R. Champness, P.H. Beton, Nature 424 (2003) 1029.
[107] L.M.A. Perdigão, E.W. Perkins, J. Ma, P.A. Staniec, B.L. Rogers, N.R. Champness, P.H. Beton, J. Phys. Chem. B 110 (2006) 12539.
[108] P.A. Staniec, L.M.A. Perdigão, A. Saywell, N.R. Champness, P.H. Beton, ChemPhysChem 8 (2007) 2177.
[109] L.A. Perdigão, A. Saywell, G.N. Fontes, P.A. Staniec, G. Goretzki, A.G. Phillips, N.R. Champness, P.H. Beton, Chem. Eur. J. 14 (2008) 7600.
[110] M.E. Cañas-Ventura, W.D. Xiao, D. Wasserfallen, K. Müllen, H. Brune, J.V. Barth, R. Fasel, Angew. Chem. Int. Ed. 46 (2007) 1814.
[111] L.M.A. Perdigão, N.R. Champness, P.H. Beton, Chem. Commun. (2006) 538.
[112] W. Xu, M.D. Dong, H. Gersen, E. Rauls, S. Vázquez-Campos, M. Crego-Calama, D.N. Reinhoudt, I. Stensgaard, E. Laegsgaard, T.R. Linderoth, F. Besenbacher, Small 3 (2007) 854.
[113] E. Barrena, D.G.D. Oteyza, H. Dosch, Y. Wakayama, ChemPhysChem 8 (2007) 1915.
[114] N. Lin, A. Langner, S.L. Tait, C. Rajadurai, M. Ruben, K. Kern, Chem. Commun. (2007) 4860.
[115] S. Weigelt, C. Busse, C. Bombis, M.M. Knudsen, K.V. Gothelf, T. Strunskus, C. Wöll, M. Dahlbom, B. Hammer, E. Lœsgaard, F. Besenbacher, T.R. Linderoth, S. Weigelt, Angew. Chem. Int. Ed. 46 (2007) 9227.
[116] G. Otero, G. Biddau, C. Sánchez-Sánchez, R. Caillard, M.F. López, C. Rogero, F.J. Palomares, N. Cabello, M.A. Basanta, J. Ortega, J. Mendez, A.M. Echavarren, R. Perez, B. Gomez-Lor, J.A. Martin-Gago, Nature 454 (2008) 865.
[117] X. Shao, X. Luo, X. Hu, K. Wu, J. Phys. Chem. B 110 (2006) 1288.
[118] D. Wang, L.J. Wan, J. Phys. Chem. C 111 (2007) 16109.
[119] S.L. Tait, A. Langner, N. Lin, R. Chandrasekar, O. Fuhr, M. Ruben, K. Kern, Chem. Phys. Chem. 9 (2008) 2495.
[120] M. Lackinger, S. Griessl, W.M. Heckl, M. Hietschold, G.W. Flynn, Langmuir 21 (2005) 4984.
[121] W. Mamdouh, H. Uji-i, J.S. Ladislaw, A.E. Dulcey, V. Percec, F.C. De Schryver, S. De Feyter, J. Am. Chem. Soc. 128 (2006) 317.
[122] L. Kampschulte, T.L. Werblowsky, R.S.K. Kishore, M. Schmittel, W.M. Heckl, M. Lackinger, J. Am. Chem. Soc. 130 (2008) 8502.
[123] M. Pokrifchak, T. Turner, I. Pilgrim, M.R. Johnston, K.W. Hipps, J. Phys. Chem. C 111 (2007) 7735.
[124] N. Wintjes, D. Bonifazi, F.Y. Cheng, A. Kiebele, M. Stöhr, T. Jung, H. Spillmann, F. Diederich, Angew. Chem. Int. Ed. 46 (2007) 4089.
[125] H.L. Zhang, W. Chen, H. Huang, L. Chen, A.T.S. Wee, J. Am. Chem. Soc. 130 (2008) 2720.
[126] S. Stepanow, N. Lin, J.V. Barth, K. Kern, Chem. Commun. (2006) 2153.
[127] A. Kiebele, D. Bonifazi, F.Y. Cheng, M. Stöhr, F. Diederich, T. Jung, H. Spillmann, ChemPhysChem 7 (2006) 1462.
[128] S. Yoshimoto, E. Tsutsumi, R. Narita, Y. Murata, M. Murata, K. Fujiwara, K. Komatsu, O. Ito, K. Itaya, J. Am. Chem. Soc. 129 (2007) 4366.
[129] H. Spillmann, A. Kiebele, M. Stöhr, T.A. Jung, D. Bonifazi, F. Cheng, F. Diederich, Adv. Mater. 18 (2006) 275.
[130] R. Madueno, M.T. Räisänen, C. Silien, M. Buck, Nature 454 (2008) 618.
[131] S. Yoshimoto, Y. Honda, O. Ito, K. Itaya, J. Am. Chem. Soc. 130 (2008) 1085.
[132] W.D. Xiao, D. Passerone, P. Ruffieux, K. Aït-Mansour, O. Gröning, E. Tosatti, J.S. Siegel, R. Fasel, J. Am. Chem. Soc. 130 (2008) 4767.
[133] D. Bléger, D. Kreher, F. Mathevet, A.-J. Attias, G. Schull, A. Huard, L. Douillard, C. Fiorini-Debuischert, F. Charra, Angew. Chem. Int. Ed. 46 (2007) 7404.
[134] D. Écija, R. Otero, L. Sánchez, J.M. Gallego, Y. Wang, M. Alcamí, F. Martín, N. Martín, R. Miranda, Angew. Chem. Int. Ed. 46 (2007) 7874.
[135] Y.H. Liu, S.B. Lei, S.X. Yin, S.L. Xu, Q.Y. Zheng, Q.D. Zeng, C. Wang, L.J. Wan, C.L. Bai, J. Phys. Chem. B 106 (2002) 12569.
[136] S.B. Lei, K. Tahara, X.L. Feng, S. Furukawa, F.C. De Schryver, K. Müllen, Y. Tobe, S. De Feyter, J. Am. Chem. Soc. 130 (2008) 7119.
[137] J.A. Theobald, N.S. Oxtoby, N.R. Champness, P.H. Beton, T.J.S. Dennis, Langmuir 21 (2005) 2038.
[138] G. Schull, L. Douillard, C. Fiorini-Debuisschert, F. Charra, F. Mathevet, D. Kreher, A.-J. Attias, Nano Lett. 6 (2006) 1360.
[139] B. Hulsken, R. Van Hameren, J.W. Gerritsen, T. Khoury, P. Thordarson, M.J. Crossley, A.E. Rowan, R.J.M. Nolte, J.A.A.W. Elemans, S. Speller, Nat. Nanotechnol. 2 (2007) 285.
[140] K. Kim, W.S. Jeon, J.-K. Kang, J.W. Lee, S.Y. Jon, T. Kim, K. Kim, Angew. Chem. Int. Ed. 42 (2003) 2293.
[141] S.J. Lee, S.-H. Cho, K.L. Mulfort, D.M. Tiede, J.T. Hupp, S.T. Nguyen, J. Am. Chem. Soc. 130 (2008) 16828.